Munc18-1 domain-1 controls vesicle docking and secretion by interacting with syntaxin-1 and chaperoning it to the plasma membrane

Gayoung A. Han[a,b], Nancy T. Malintan[c], Ner Mu Nar Saw[a,b], Lijun Li[a], Liping Han[a,b], Frederic A. Meunier[c], Brett M. Collins[d], and Shuzo Sugita[a,b]

[a]Division of Fundamental Neurobiology, University Health Network, Toronto ON M5T 2S8, Canada; [b]Department of Physiology, University of Toronto, Toronto ON M5S 1A8, Canada; [c]Queensland Brain Institute and [d]Institute for Molecular Bioscience, University of Queensland, Brisbane, Australia 4072

ABSTRACT **Munc18-1 plays pleiotropic roles in neurosecretion by acting as 1) a molecular chaperone of syntaxin-1, 2) a mediator of dense-core vesicle docking, and 3) a priming factor for soluble *N*-ethylmaleimide–sensitive factor attachment protein receptor–mediated membrane fusion. However, how these functions are executed and whether they are correlated remains unclear. Here we analyzed the role of the domain-1 cleft of Munc18-1 by measuring the abilities of various mutants (D34N, D34N/M38V, K46E, E59K, K46E/E59K, K63E, and E66A) to bind and chaperone syntaxin-1 and to restore the docking and secretion of dense-core vesicles in Munc18-1/-2 double-knockdown cells. We identified striking correlations between the abilities of these mutants to bind and chaperone syntaxin-1 with their ability to restore vesicle docking and secretion. These results suggest that the domain-1 cleft of Munc18-1 is essential for binding to syntaxin-1 and thereby critical for its chaperoning, docking, and secretory functions. Our results demonstrate that the effect of the alleged priming mutants (E59K, D34N/M38V) on exocytosis can largely be explained by their reduced syntaxin-1–chaperoning functions. Finally, our data suggest that the intracellular expression and distribution of syntaxin-1 determines the level of dense-core vesicle docking.**

Monitoring Editor
Benjamin Glick
University of Chicago

Received: Feb 15, 2011
Revised: Aug 22, 2011
Accepted: Aug 30, 2011

INTRODUCTION

Sec1/Munc18 (SM) proteins are highly conserved 60- to 70-kDa polypeptides that are indispensable regulators of membrane fusion through their roles in soluble *N*-ethylmaleimide–sensitive factor attachment protein receptor (SNARE) trafficking and complex formation (Rizo and Südhof, 2002; Toonen and Verhage, 2007; Südhof and Rothman, 2009; Han *et al.*, 2010). Polypeptide chains of Munc18 consist of three different domains: domain-1, -2, and -3 (3a, 3b; Misura *et al.*, 2000; Figure 1A). In mammals, there are three Munc18 isoforms, Munc18-1, -2, and -3 (also called Munc18a, b, c). Munc18-1 is expressed primarily in neurons and neuroendocrine cells (Hata *et al.*, 1993; Garcia *et al.*, 1994; Pevsner *et al.*, 1994); Munc18-2 in, contrast, is expressed in numerous cell types with the exception of the brain, and Munc18-3 is expressed ubiquitously (Hata and Südhof, 1995; Katagiri *et al.*, 1995; Tellam *et al.*, 1995; Halachmi and Lev, 1996; Riento *et al.*, 1996). When Munc18-1 was first isolated, it was initially found to tightly bind the target-SNARE syntaxin-1 (Hata *et al.*, 1993). Since then, the specificity of binding between Munc18 and the various syntaxin isoforms has been studied extensively; Munc18-1 and -2 can bind to syntaxin-1A, -1B, -2, and -3, whereas Munc18-3 binds to syntaxin-2 and -4 (Hata and Südhof, 1995; Tellam et al., 1995, 1997; Halachmi and Lev, 1996; Riento *et al.*, 1998, 2000; Tamori *et al.*, 1998; Kauppi *et al.*, 2002; Latham *et al.*, 2006; Hu *et al.*, 2007).

The importance of Munc18-1 and its orthologues (Unc-18 in *Caenorhabditis elegans*, Rop in *Drosophila*) in exocytosis/membrane fusion has been clearly established through the complete or near-complete lack of neurotransmitter-release phenotypes seen in these null mutants (Hosono *et al.*, 1992; Schulze *et al.*, 1994; Verhage *et al.*, 2000; Weimer *et al.*, 2003). Nonetheless, the precise modality of Munc18-1 in the process of exocytosis is still poorly understood.

This article was published online ahead of print in MBoC in Press (http://www.molbiolcell.org/cgi/doi/10.1091/mbc.E11-02-0135) on September 7, 2011.

Address correspondence to: Shuzo Sugita (ssugita@uhnres.utoronto.ca).

Abbreviations used: EmGFP, Emerald green fluorescent protein; ITC, isothermal titration calorimetry; mint-1, Munc18-interacting protein; SNARE, soluble *N*-ethylmaleimide–sensitive factor attachment protein receptor; SNM, silent nucleotide mutations; WT, wild type.

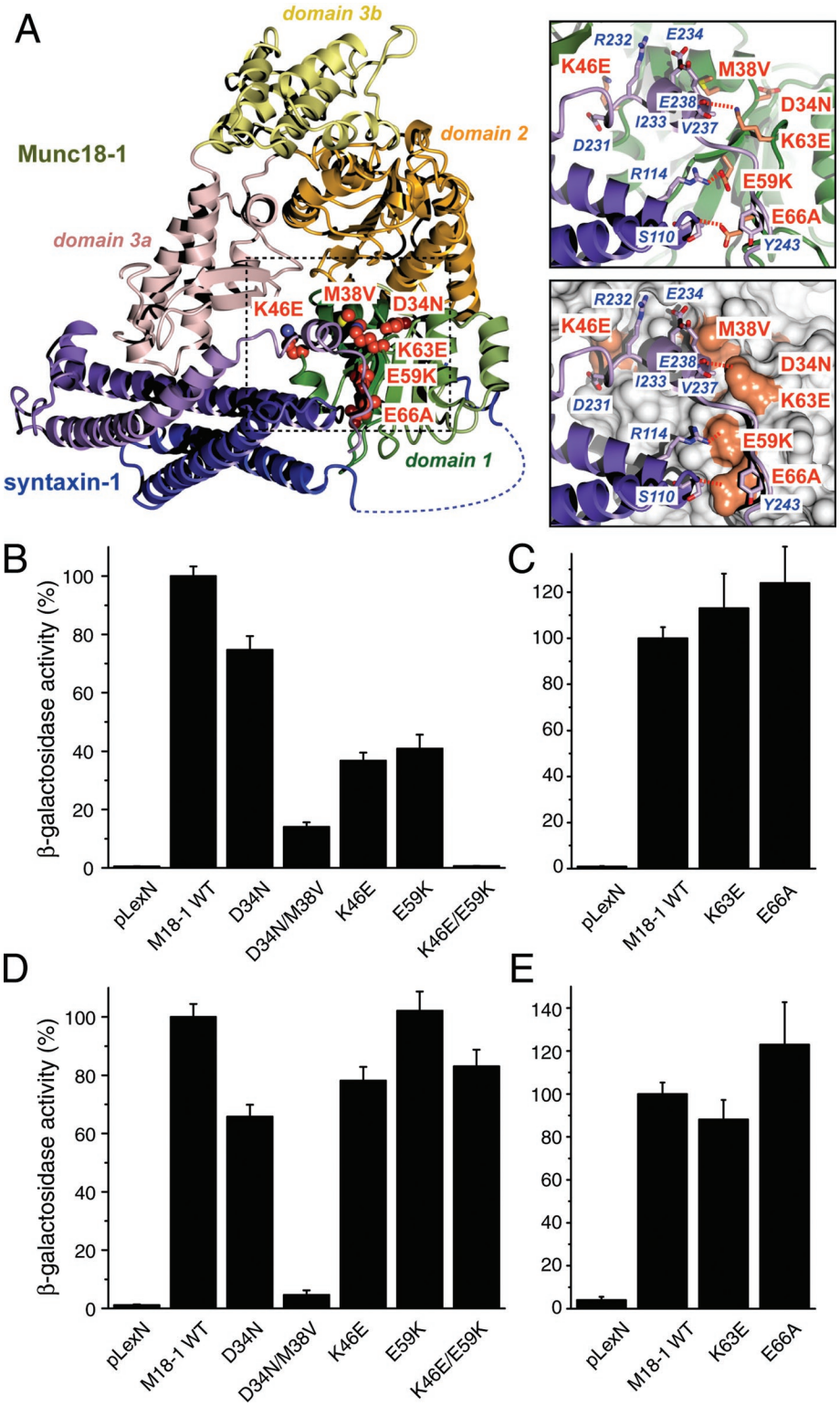

FIGURE 1: Mutations in domain-1 of Munc18-1 result in reductions in the binding to syntaxin-1. (A) Structure of the Munc18-1/syntaxin-1 complex (Burkhardt *et al.*, 2008), highlighting domain-1 mutations studied here. Each domain of Munc18-1 is represented in a different color. Domain-1 is displayed in green, and the mutated residues are indicated in orange. Syntaxin-1 is represented in dark blue and purple. The binding between these Munc18-1 mutants (D34N, D34N/M38V, K46E, E59K, and K46E/E59K) and (B) syntaxin-1A or (D) mint-1 was analyzed by yeast two-hybrid assays. The binding between Munc18-1 mutants K63E and E66A and (C) syntaxin-1A or (E) mint-1 was also analyzed by yeast two-hybrid assays. In each assay, β-galactosidase activities of the transformed yeast clones were quantified (*Materials and Methods*) and normalized so that the activity of the yeast clones transformed with the wild-type Munc18-1 was set to 100%. Error bars indicate SEM (n = 11–12 for binding to syntaxin-1; n = 11–12 for binding to mint-1). Note that K46E/E59K mutation in Munc18-1 abolished the binding to syntaxin-1 but not that to mint-1. D34N/M38V mutation in Munc18-1 lost the binding to both syntaxin-1 and mint-1.

At least three important functions of Munc18-1 have been proposed and supported with substantial (although sometimes contradictory) experimental evidence (Han *et al.*, 2010): 1) molecular chaperone of syntaxin-1, allowing proper expression of syntaxin-1 at the plasma membrane (Rowe *et al.*, 1999, 2001; Medine *et al.*, 2007; Arunachalam *et al.*, 2008; McEwen and Kaplan, 2008; Han *et al.*, 2009; Malintan *et al.*, 2009); 2) priming via promotion of SNARE complex–mediated membrane fusion (Shen *et al.*, 2007a, 2010; Rodkey *et al.*, 2008; Tareste *et al.*, 2008; Südhof and Rothman, 2009); and 3) docking of large, dense-core vesicles to the plasma membrane (Voets *et al.*, 2001; Toonen *et al.*, 2006).

Moreover, at least three binding modes of Munc18 with its cognate syntaxin or with the SNARE complex have been proposed. The binary interaction between the "closed" conformation of syntaxin-1 and Munc18-1 was the first binding mode discovered (Hata *et al.*, 1993; Misura *et al.*, 2000). This interaction is mediated by domain-1 and -3a of Munc18-1; the central cavity formed by these domains provides the binding cleft for syntaxin-1 in an autoinhibited conformation. Some of the key residues that make specific contact with "closed" syntaxin lie in the surface (largely formed by residues 38–71) of domain-1 and the residues 271–280 and 331–338 of domain-3a (Misura *et al.*, 2000). This binary interaction has been reported to be important for the chaperoning function of Munc18-1 by preventing the formation of ectopic SNARE complexes (Medine *et al.*, 2007; Arunachalam *et al.*, 2008; Han *et al.*, 2009; Malintan *et al.*, 2009). The importance of Munc18-1's domain-1 in its binary interaction with syntaxin-1 and its chaperoning and secretory functions has recently been inferred from the phenotype of the K46E/E59K double mutant. This Munc18-1 mutant loses its ability to bind and chaperone syntaxin-1 and to restore secretion in Munc18-1/-2 double-knockdown PC12 cells (Han *et al.*, 2009). A second binding mode is mediated by the interaction between the N-terminal peptide (residues 1–20) of syntaxin-1 and the

hydrophobic pocket (residues 110–134) in domain-1 of Munc18-1. This binding mode appears to mediate the interaction between Munc18-1 and the SNARE complex (Rickman *et al.*, 2007; Shen *et al.*, 2007a; Rathore *et al.*, 2010), which was proposed to underlie the stimulation of SNARE-mediated membrane fusion by Munc18-1 (Shen *et al.*, 2007a; Südhof and Rothman, 2009). A third binding mode suggests that Munc18-1 binds to the assembled SNARE complex other than through the binding to syntaxin-1 N-terminal peptide (Dulubova *et al.*, 2007; Latham and Meunier, 2007; Shen *et al.*, 2007b; Rodkey *et al.*, 2008; Xu *et al.*, 2010). Moreover, Munc18-1 was recently shown to associate with syntaxin-1 via the N-terminal peptide but adopts an alternative conformation by which Munc18-1 domain-3 extends and precludes "closed" syntaxin-1 binding (Hu *et al.*, 2011). This possible change in conformation of helical hairpin structure of domain-3a, which might play a role in releasing syntaxin-1 from the Munc18-1/syntaxin-1 complex, was suggested through analysis of the homologous squid Sec1 structure (Bracher *et al.*, 2000; Bracher and Weissenhorn, 2001). This extended domain-3 may present a platform for the assembly of the SNARE complex; however, this remains to be confirmed.

Although the pleiotropic roles of Munc18-1 in neurosecretion are supported by multiple lines of evidence, it is unclear how these functions are correlated and executed. Perhaps the most puzzling conclusion from these studies is that similar or identical residues in the domain-1 cleft of Munc18-1 are considered to play critical roles in both the chaperoning and the priming function of Munc18-1. Specifically, three different mutants (D34N/M38V, E59K, and E66A) in the domain-1 cleft have been proposed to represent "priming" mutants. These mutants are believed to be impaired in their ability to promote priming/exocytosis while maintaining the syntaxin-1 chaperoning function. In addition, a homologous mutation to E59K in Vps33, a yeast SM protein, was proposed to cause a defect in fusion pore opening (Pieren *et al.*, 2010), although the role of Munc18-1 in the opening of the fusion pore is highly controversial (Voets *et al.*, 2001). The D34N/M38V mutant has been shown to impair binary binding to syntaxin-1 and disrupt the docking of dense-core vesicles. Of importance, this mutant was capable of restoring syntaxin-1 distribution to the plasma membrane, which suggested that the D34N/M38V mutant was specifically a priming mutant (Gulyás-Kovács *et al.*, 2007). It was, however, unclear how a mutant shown to lose its binary binding to syntaxin-1 could maintain its chaperoning function, which is known to mainly rely on this interaction (Gulyás-Kovács *et al.*, 2007). Unlike D34N/M38V, the E59K mutation was shown to maintain the binary binding to syntaxin-1 to a significant extent while abolishing the binding to the SNARE complex (Deák *et al.*, 2009). In addition, the E66A mutant was also shown to have intact binary binding to syntaxin-1 but decreased binding to SNARE complex, although not as severely impaired as that of the E59K mutant. The differential effects of these mutations on SNARE complex binding were suggested to correlate with the defects in synaptic vesicle priming and neurotransmitter release (Deák *et al.*, 2009). Glu59 was suggested to be a critical residue for binding to closed syntaxin-1 (Misura *et al.*, 2000; Kauppi *et al.*, 2002; Han *et al.*, 2009), but whether the E59K mutant of Munc18-1 retains its chaperoning function has not yet been examined. Thus it is unclear whether these priming mutants retain a normal level of syntaxin-1–chaperoning function and/or whether diminished secretion in these mutants is caused by their reduced syntaxin-1–chaperoning function or their reduced priming function.

In an attempt to clarify the specific function of the domain-1 cleft of Munc18-1 in neurosecretion and to further characterize the phenotypes of previously proposed priming mutants, we investigated various domain-1 cleft mutants (K46E, E59K, K46E/E59K, K63E, E66A, D34N, and D34N/M38V) in detail by employing a combination of biochemical and physiological analyses. We discovered striking correlations between the abilities of these mutants to bind and chaperone syntaxin-1 and their abilities to restore vesicle docking and secretion. Our results demonstrate that domain-1 of Munc18-1 is essential for high-affinity syntaxin-1 interaction and consequently critical for its syntaxin-1–chaperoning, vesicle docking, and secretory functions. Furthermore, our data suggest that the effect of previously proposed priming mutants (E59K, D34N/M38V) on exocytosis is better explained by their reduced syntaxin-1 chaperoning functions.

RESULTS

Lys-46 and Glu-59 are critical for the binary interaction between Munc18-1 and syntaxin-1

Three mutants (D34N/M38V, E59K, and E66A) in the domain-1 cleft of Munc18-1 have been proposed to selectively abrogate Munc18-1's priming function with limited or no effects on its chaperoning function of syntaxin-1 (Gulyás-Kovács *et al.*, 2007; Deák *et al.*, 2009). It is surprising, however, that these mutants have different characteristics in their ability to bind to syntaxin-1. The D34N/M38V mutant binds poorly to syntaxin-1 (measured by glutathione *S*-transferase [GST] pull-down; Gulyás-Kovács *et al.*, 2007), whereas the E59K and E66A mutants have limited (E59K) or no effect (E66A) on binding to syntaxin-1 (measured by isothermal titration calorimetry (ITC)) (Deák *et al.*, 2009). We therefore reexamined the ability of these mutants, together with other single or double mutants (D34N, K46E, K46E/E59K, and K63E) in the domain-1 cleft, to bind to syntaxin-1. Lys-46 of Munc18-1 specifically contacts residues Asp-231 and Arg-232 in the H3 helix of syntaxin-1, and Glu-59 of Munc18-1 forms a buried salt bridge with Arg-114 within the H3 domain of syntaxin-1 when in the closed conformation (Figure 1A). Lys-63 of Munc18-1 contacts the SNARE motif of syntaxin-1, and the Glu-66 residue of Munc18-1 contacts both Habc and the SNARE motif of syntaxin-1 (Deák *et al.*, 2009). Although Asp34 was suggested to form evolutionary conserved hydrogen bond interactions with the syntaxin N-terminal Habc domain and thus is necessary for syntaxin-1 binding (Gulyás-Kovács *et al.*, 2007), specific syntaxin-1 residues that interact with Asp-34 of Munc18-1 are not observed in the crystal structure (Misura *et al.*, 2000) (Figure 1A). The residue Met-38 forms a hydrophobic contact with C-terminal regions of the syntaxin-1 protein, specifically interacting with aliphatic regions of syntaxin-1 residues Glu-234, Glu-238, Val-237, and Ile-233.

To examine the binding between Munc18-1 mutants and the cytoplasmic domain of syntaxin-1, we first performed yeast two-hybrid assays. This assay is an unbiased method to examine protein–protein interactions. It provides a more in vivo–like environment for binding interactions to occur (Vojtek *et al.*, 1993; Han *et al.*, 2009). To ensure that domain-1 mutants specifically lose their ability to bind to syntaxin-1, we used mint-1 (Munc18-interacting protein; Okamoto and Südhof, 1997) as a control and examined the interaction between this protein and the Munc18-1 mutants. Single mutants of K46E or E59K significantly reduced binding to syntaxin-1, whereas a double mutation of K46E/E59K completely abolished the binding to syntaxin-1 (Figure 1B). Despite reduced syntaxin-1 binding, all three mutants maintained normal levels of mint-1 binding (Figure 1D). These results imply that K46E and E59K single mutants and K46E/E59K double mutant selectively lose their ability to bind to syntaxin-1. In contrast, the K63E and E66A single mutants retained their ability to bind to both syntaxin-1 and mint-1 (Figure 1, C and E).

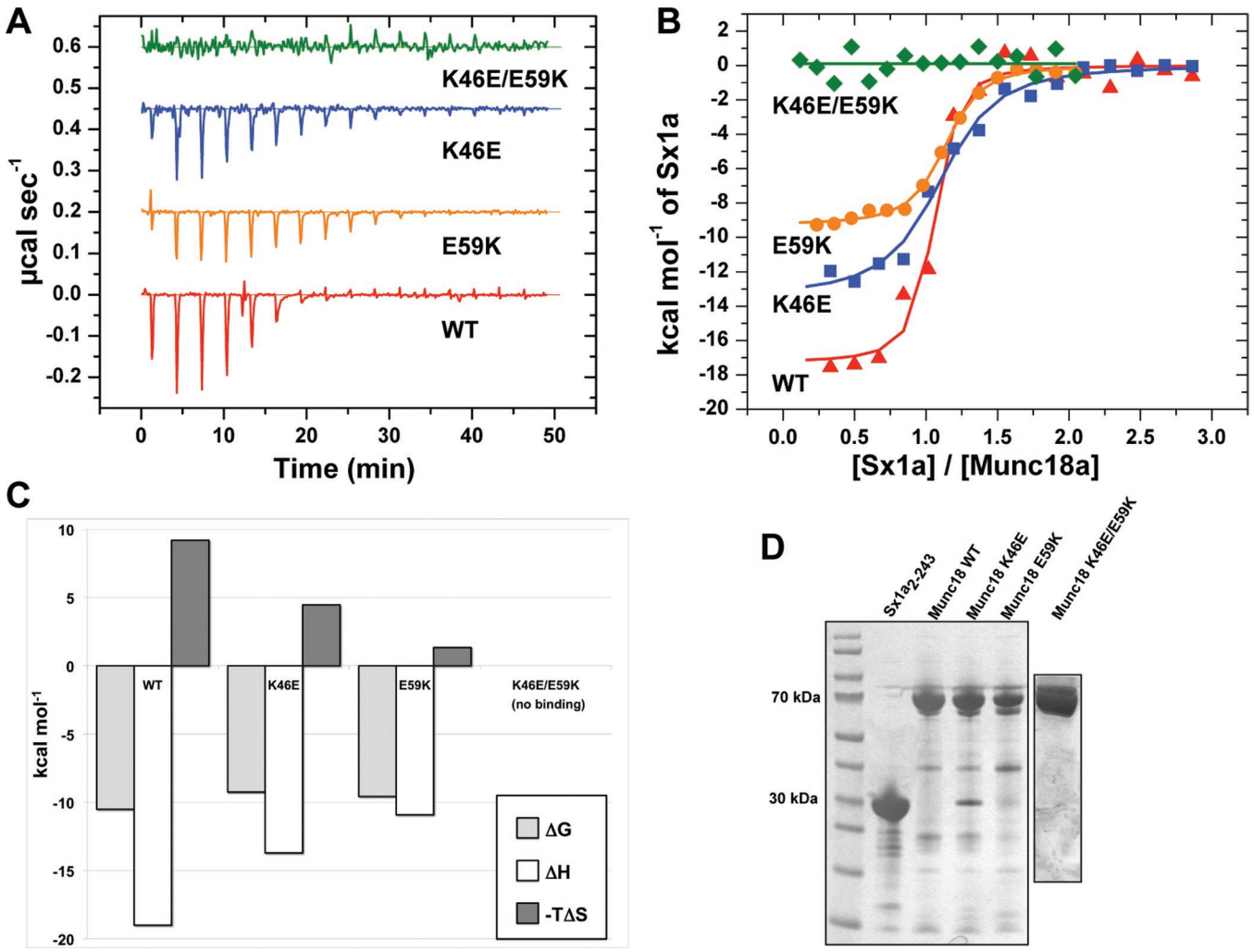

FIGURE 2: ITC analysis of the binding of $Sx1a_{2\text{-}243}$ to Munc18-1. (A) Representative raw ITC data for binding of Munc18-1 WT, K46E, E59K, and K46E/E59K variants to $Sx1a_{2\text{-}243}$. (B) Integrated and normalized ITC data for the same experiments as shown in A. (C) The thermodynamic parameters of Munc18-1 binding (Table 1) are plotted to highlight the changes in binding enthalpy of the different Munc18-1 mutants. (D) Coomassie-stained SDS polyacrylamide gel of the proteins used in ITC experiments.

The D34N mutant exhibited slightly reduced binding to syntaxin-1 (Figure 1B), whereas D34N/M38V double mutations caused a dramatic reduction in binding to syntaxin-1 (Figure 1B), which is consistent with the previous GST pull-down experiments (Gulyás-Kovács *et al.*, 2007). Unexpectedly, however, the D34N/M38V mutant also abolished the interaction with mint-1 (Figure 1D), suggesting that the D34N/M38V double mutant appears to lose its binding ability not only to syntaxin-1, but to other interactors as well. This implies that the D34N/M38V mutation may affect the folding or expression level of Munc18-1. As shown in Figure 9 later in this paper, we noticed that the expression level of the D34N/M38V mutant was unusually low compared with that of the other mutants in PC12 cells, suggesting that there is a possibility that this mutation has affected the expression level of this protein. Albeit to a lesser degree, the D34N mutant also showed a reduced expression level (Figure 9). Therefore we initially focused our efforts on reevaluating the E59K mutant, together with K46E and K46E/E59K mutants.

Previous experiments using ITC showed that the E59K mutation reduced binding affinity to syntaxin-1, although this effect did not reach a statistically significant level. The thermodynamic parameters were also significantly altered, with a much reduced enthalpic contribution to the association (Deák *et al.*, 2009). Our yeast two-hybrid data revealed a significant reduction in binding to syntaxin-1 for the E59K mutant (Figure 1B). Therefore, to further characterize the interaction between Munc18-1 domain-1 mutants and syntaxin-1, we performed ITC experiments to measure the affinity between a cytoplasmic domain of syntaxin-1A and domain-1 cleft mutants: K46E, E59K, and K46E/E59K (Figure 2 and Table 1). In brief, all ITC results were consistent with our yeast two-hybrid data. We found significant reductions in the binding enthalpy (ΔH) for both K46E and E59K single mutants (−19.0 ± 1.98 kcal/mol, n = 3, for the wild type [WT] vs. −13.7 ± 0.21 kcal/mol, n = 3, for K46E; and −11.5 ± 1.17 kcal/mol, n = 4, for E59K; $p < 0.01$ for both mutants; Figure 2, B and C; Table 1). The dissociation constants (K_d) of K46E and E59K mutants binding to syntaxin-1 were significantly increased compared with that of the corresponding WT (181.2 ± 46.4 nM for $K46E{:}Syx1a_{2\text{-}243}$ and 83.9 ± 34.3 nM for $E59K{:}Sx1a_{2\text{-}243}$ vs. 23.3 ± 11.1 nM for $WT{:}Syx1a_{2\text{-}243}$; $p < 0.01$ for K46E and $p < 0.05$ for E59K), which indicates reduced binding affinities of the single mutants (Table 1). When these two residues were mutated simultaneously (K46E/E59K double mutations), no binding was observed under the sample conditions used here, confirming the data from the yeast

Munc18 protein	ΔH (kcal mol^{-1})	−TΔS (kcal mol^{-1})	ΔG (kcal mol^{-1})	K_d (nM)	N
WT	−19.0 ± 1.98	8.6 ± 1.73	−10.5 ± 0.25	23.3 ± 11.1	1.0 ± 0.01
K46E	−13.7 ± 0.21**	4.5 ± 0.11**	−9.2 ± 0.11**	181.2 ± 46.4**	1.0 ± 0.06
E59K	−11.5 ± 1.17**	1.8 ± 0.94**	−9.7 ± 0.26**	83.9 ± 34.3*	1.1 ± 0.10
K46E/E59K	No binding signal	—	—	—	—

Values are expressed as means ± SD (n = 3–4). All experiments were performed at 298 K. Significant at *p < 0.05, **p < 0.01.

TABLE 1: Binding parameters of Munc18-1 interaction with $Sx1a_{2\text{-}243}$.

two-hybrid assay (Figures 1B and 2B and Table 1). These results indicate that the single point mutations in the domain-1 cleft of Munc18-1 (K46E and E59K) significantly affect the thermodynamics and affinity of association, whereas the combined mutation K46E/E59K essentially abolishes the association. The consistency of the ITC experiments (Figure 2 and Table 1) and the results of the yeast two-hybrid assay (Figure 1) provide confidence that these mutations represent a scale of reduced binding affinity in which WT > E59K ~ K46E >> K46E/E59K.

K46E, E59K, and K46E/E59K mutants show various degrees of syntaxin-1–chaperoning activity, which correlate with their ability to bind syntaxin-1

In Munc18-1/-2 double-knockdown PC12 cells the cellular level of syntaxin-1 is significantly reduced and the localization of syntaxin-1 to the plasma membrane is abolished (Han *et al.*, 2009). These phenotypes can be rescued by expression of exogenous wild-type Munc18-1. After observing that point mutations in the domain-1 cleft reduced Munc18-1's binding ability to syntaxin-1 to various extents, we examined the abilities of these mutants to rescue syntaxin-1 expression and localization in the Munc18-1/-2 double-knockdown cells. We fused the domain-1 mutants with Emerald green fluorescent protein (EmGFP; Munc18-1–EmGFP) and expressed them stably using the *Lentivirus* system in the Munc18-1/-2 double-knockdown PC12 cells (clones D7 and D16; Han *et al.*, 2009). The expression plasmid contains the IRES-blasticidin resistance gene, which enabled the selection of the infected cells. The recombinant virus was applied to D7 and D16 cells, and the infected cells were isolated. The expression level of Munc18-1–EmGFP proteins was verified by immunoblot analysis using anti–Munc18-1 antibody. Syntaxin-1 expression levels upon introduction of various recombinant Munc18-1 mutants were probed by immunocytochemistry using an anti–syntaxin-1 antibody.

In both D7 and D16 cells, Munc18-1 K46E, E59K, and K46E/E59K mutants were expressed at a comparable level to the endogenous Munc18-1 in wild-type PC12 cells. Moreover, these mutants were expressed at a similar level to the exogenous wild-type Munc18-1 fused with EmGFP in double-knockdown PC12 cells (Figure 3). Of importance, in both lines of double-knockdown clones (D7 and D16), the exogenous expression of wild-type Munc18-1–EmGFP resulted in a dramatic recovery of syntaxin-1 expression comparable to that of endogenous syntaxin-1 present in wild-type PC12 cells. On expression of the single mutants K46E or E59K, syntaxin-1 expression was rescued, although less efficiently than in wild-type Munc18-1–EmGFP–expressing cells. In the case of the K46E/E59K double mutant, there was very little rescue of the reduced syntaxin-1 expression level, which remained at a low level comparable to the control EmGFP vector alone (Figure 3, A and B). The expression levels of these mutant proteins were comparable to those of the wild-type Munc18-1–EmGFP protein, and therefore the reduced ability of the mutants to rescue syntaxin-1 expression is not simply due to decreased levels of protein. This strongly advocates for a role of Munc18-1 and syntaxin-1 interaction in stabilizing the expression and distribution of syntaxin-1. Considering the strong effect of Munc18-1 E59K mutation on syntaxin-1 expression, it is highly likely that this mutation affects the syntaxin-1–chaperoning function of Munc18-1, which had not been addressed previously (Deák *et al.*, 2009).

The rescue of syntaxin-1 expression by Munc18-1 mutants is in the order of WT > E59K ~ K46E > K46E/E59K (Figure 3, A and B), which coincides with the order of their binding affinity to syntaxin-1 (Figures 1 and 2). Therefore we examined the correlation between the binding affinity of Munc18-1 mutants to syntaxin-1 and their ability to restore syntaxin-1 expression. We used the equilibrium association constant K_a (= K_d^{-1}) as an index of binding affinity, and the value of each mutant was normalized such that WT was set to be 1. We quantified the recovery of syntaxin-1 expression from the chemiluminescence signal for the respective Munc18-1–EmGFP protein using Image J and normalized (set to 1 and 0 for syntaxin-1 expression in PC12 DKD expressing Munc18-1-WT–EmGFP and EmGFP, respectively). We found a striking correlation (r^2 = 0.93, n = 8) between these two parameters, which is highly significant ($p < 0.001$; Figure 3C). This result indicates that the binding affinity of Munc18-1 mutants to syntaxin-1 and their ability to restore syntaxin-1 expression are positively correlated.

We further examined the ability of the Munc18 mutants to rescue the mislocalization of syntaxin-1 in Munc18-1/-2 double–knockdown D16 cells by using confocal immunofluorescence microscopy (Figure 4). As previously reported (Han *et al.*, 2009; Malintan *et al.*, 2009), the plasma membrane localization of syntaxin-1 was recovered upon expression of the wild-type Munc18-1–EmGFP. Syntaxin-1 remained in the perinuclear region of the cells upon expression of empty vector containing only EmGFP (Figure 4, A and B). Expression of either Munc18-1 K46E or E59K single mutant showed a limited level of rescue of syntaxin-1 on the plasma membrane as compared with cells expressing the wild-type Munc18-1–EmGFP. The perinuclear localization and the apparent plasma localization of syntaxin-1 seemed to coexist in the cells expressing K46E or E59K single mutant, although perinuclear accumulation of syntaxin-1 was more prominent (Figure 4, C and D). In the case of K46E/E59K–EmGFP double-mutant–expressing cells, syntaxin-1 remained limited to the perinuclear region of the cells, indicating the complete inability of the double mutant to restore proper syntaxin-1 localization (Figure 4E). Similar results were obtained for D7 cells (Supplemental Figure S1). These results suggest that the K46E/E59K mutant loses its ability to support expression and plasma membrane localization of syntaxin-1, demonstrating the importance of these domain-1 combined residues as being critical for binding to the closed conformation of syntaxin-1. Furthermore, the differences in the extent to which these Munc18-1 variants restore syntaxin-1 expression and localization show a clear correlation with the abilities of these mutants to bind to syntaxin-1 (Figures 1 and 2) and to rescue

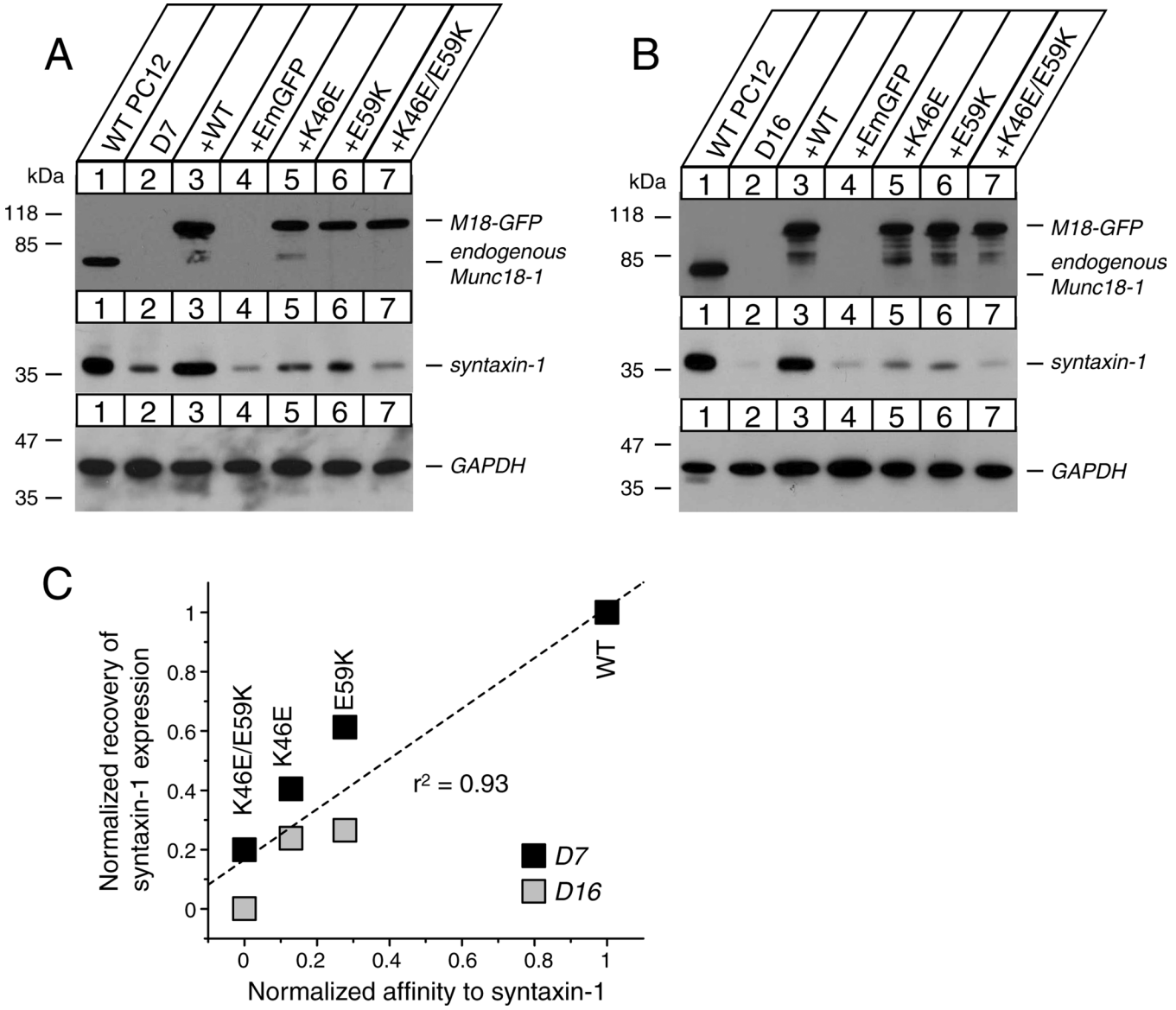

FIGURE 3: Stable reexpression of Munc18-1 variants in Munc18-1/-2 double-knockdown PC12 cells (D7 and D16) results in different degrees of recovery of syntaxin-1 expression. (A, B) Munc18-1/-2 double-knockdown clones (D7 and D16) were infected with lentiviruses that express EmGFP, wild-type Munc18-1-EmGFP, or Munc18-1 mutants (K46E, E59K, and K46E/E59K), and the infected cells were selected with blasticidin. A number on the left indicates the position of a molecular weight marker. (C) The correlation graph demonstrates that the degree of the binary interaction between Munc18-1 variants and syntaxin-1 is positively correlated with the ability of the mutants to rescue syntaxin-1 expression.

syntaxin-1 expression (Figure 3) and localization (Figure 4). The results thus far strongly support the idea that the strength of interaction between Munc18-1 mutants and syntaxin-1 is positively correlated with their abilities to restore the expression level and plasma membrane localization of syntaxin-1. This stresses the essential role of Munc18-1 domain-1 cleft in mediating syntaxin-1 interaction and consequently in syntaxin-1 stabilization and trafficking. Our results strongly support the hypothesis that domain-1 cleft plays an important role in chaperoning syntaxin-1 to the plasma membrane.

The docking of dense-core vesicles correlates with Munc18-1 chaperoning activity

The essential function of Munc18-1 in the docking of dense-core vesicles was first demonstrated by the electron microscopic analysis of Munc18-1–deficient adrenal chromaffin cells from Munc18-1–null mice (Voets *et al.*, 2001). The term "docking" was coined to anatomically define secretory vesicles in close apposition (within 50 nm) to the plasma membrane (Arunachalam *et al.*, 2008). In Munc18-1–knockdown PC12 cells, a significant decrease in the proportion of docked dense-core vesicles was observed (30–40% docking in the control PC12 cells vs. 15– 20% docking in Munc18-1 single-knockdown cells), which suggests deficiencies in vesicle docking in the Munc18-1–knockdown clone (Arunachalam *et al.*, 2008).

We examined the ability of Munc18-1 K46E, E59K, and K46E/E59K mutants to restore dense-core vesicle docking in Munc18-1/-2 double-knockdown D7 cells by using electron microscopy. Figure 5 shows examples of electron micrographs of these D7 cells rescued with control protein (EmGFP) and Munc18-1 wild-type and mutants. Arrows indicate the dense-core vesicles. Quantification of the dense-core vesicle distribution revealed a strong reduction in docked

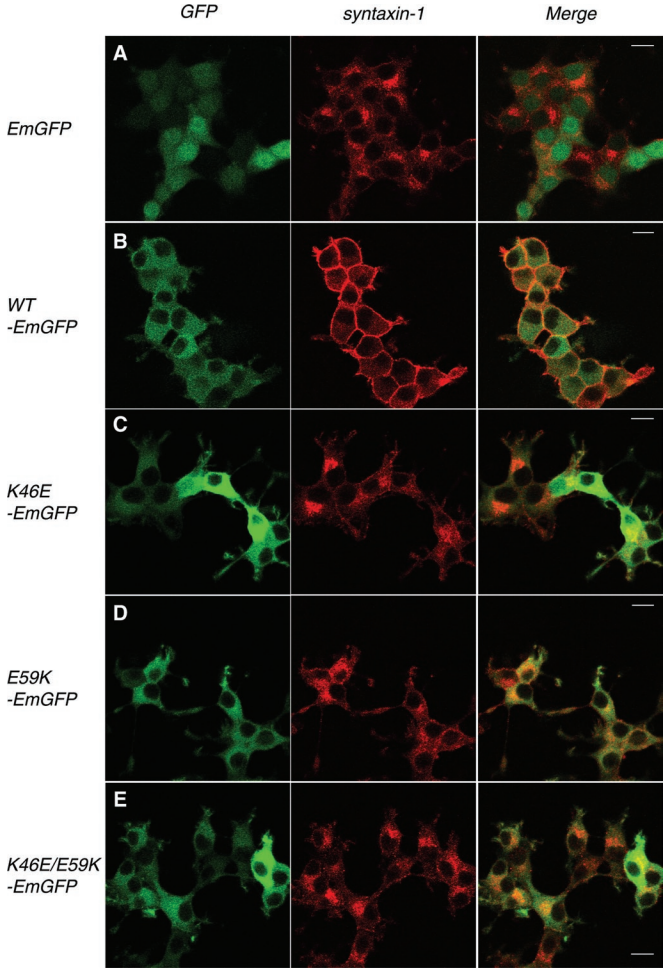

FIGURE 4: Differential rescue of syntaxin-1 localization in Munc18-1/-2 double-knockdown clone (D16) upon reintroduction of Munc18-1 variants. Confocal images of D16 cells infected with lentiviruses that express (A) negative control EmGFP alone, (B) WT Munc18-1–EmGFP, (C) K46E–EmGFP, (D) E59K–EmGFP, and (E) K46E/E59K–EmGFP (left). These cells were stained with anti-syntaxin-1 antibodies, followed by Red-X–conjugated anti-mouse antibodies (middle). Right panels are merged pictures. Bar, 10 μm.

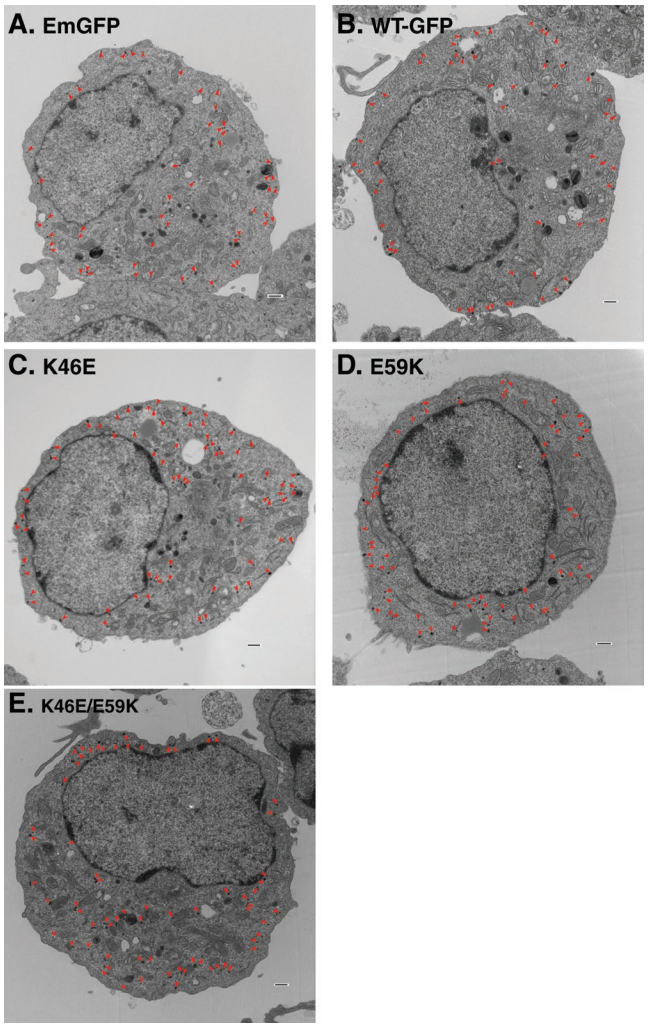

FIGURE 5: Examples of electron micrographs of Munc18-1/-2 double-knockdown cells (D7) rescued with Munc18-1 variant. Electron micrograph of a single cell from D7 rescued with (A) control protein (EmGFP), (B) WT Munc18-1–EmGFP, (C) K46E-EmGFP, (D) E59K-EmGFP, and (E) K46E/E59K–EmGFP. Dense-core vesicles are indicated by red arrows. Scale bar, 500 nm.

dense-core vesicles (i.e., vesicles within 50 nm of the plasma membrane) in knockdown PC12 cells expressing empty-EmGFP vector (7.15 ± 1.06%) compared with those expressing wild-type Munc18-1–EmGFP (24.91 ± 2.32%; Figure 6A). Munc18-1/-2 double-knockdown PC12 cells expressing either K46E or E59K showed an intermediate level of docked dense-core vesicles (13.45 ± 1.65 and 12.98 ± 1.73%, respectively). The D7 cells expressing K46E/E59K double mutant showed no rescuing activity for docking (8.30 ± 1.12%) compared with EmGFP alone. The total number of dense-core vesicles was comparable in all Munc18-1 variant–expressing cells (Figure 6B), thus excluding the possibility that the differences in the percentage of docked vesicles are affected by the total number of vesicles. We also measured the area (μm^2) of the Munc18-1/-2 double-knockdown PC12 cells expressing the Munc18-1 variants and confirmed that the morphologies of the cells have not been significantly altered in response to the expression of the mutants (Figure 6C).

We next examined the correlation between the syntaxin-1–chaperoning function of Munc18-1 and the recovery of dense-core vesicle docking. Although the chaperoning function of Munc18-1 should be evaluated not only by the restoration of syntaxin-1 expression (Figure 3), but also by the recovery of its plasma membrane localization, the latter is difficult to accurately quantify (Figure 4). Thus we used the rescue of syntaxin-1 protein levels as an index to estimate the chaperoning function of Munc18-1. We found a significant correlation ($r^2 = 0.90$) between the recovery of syntaxin-1 expression and that of dense-core vesicle docking (Figure 6D). Our results clearly indicate that the efficiency of rescue in dense-core vesicle docking in cells expressing different Munc18-1 mutants strikingly correlates with the abilities of each mutant to bind syntaxin-1 and to restore its expression level. Our results suggest that the intracellular expression and distribution of syntaxin-1 determine the level of dense-core vesicle docking.

The degree of noradrenaline-secretion rescue correlates with Munc18-1 chaperoning activity

In view of the striking correlation found between the ability of domain-1 mutants to bind syntaxin, to rescue syntaxin-1 expression and localization, and to restore the dense-core vesicle docking, we further examined the role of these domain-1 residues in neurosecretion process. We tested the ability of Munc18-1 K46E, E59K, and

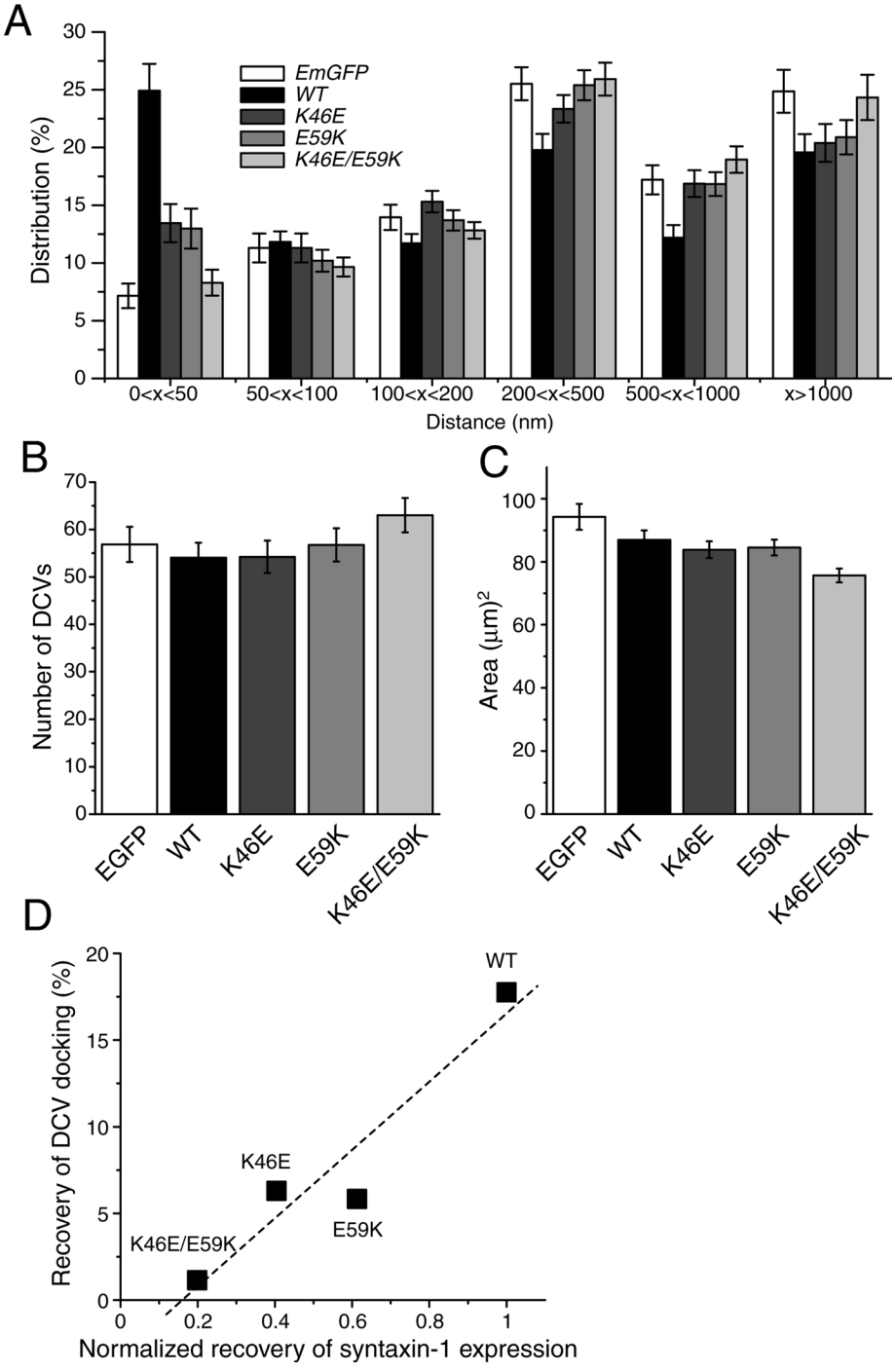

FIGURE 6: Electron microscopic analysis of dense-core vesicle distribution in the Munc18-1/-2 double-knockdown cells (D7) expressing Munc18-1 variants. (A) The mean percentage distribution of dense-core vesicles within individual PC12 cells, calculated from multiple single-cell electron micrographs. Dense-core vesicles were classed as being located within 50, 50–100, 100–200, 200–500, or 500–1000 nm or farther than 1000 nm from the plasma membrane. (B) The mean number of dense-core vesicles present in each single-cell electron micrograph from the D7 clones expressing EmGFP alone or Munc18-1 variants. (C) The mean area of each cell from D7 clones expressing EmGFP alone or Munc18-1 variants. Error bar, SEM (n = 37– 40). (D) The correlation graph demonstrates the positive correlation between the ability of the mutants to rescue syntaxin-1 expression and to restore dense-core vesicle docking efficiency.

K46E/E59K mutants to restore regulated secretion in Munc18-1/-2 double-knockdown cells. Preloaded [^{3}H]noradrenaline ([^{3}H]NA) release was stimulated by 70 mM KCl for 15 min, and a robust recovery of secretion was observed in PC12 double-knockdown cells (D7 and D16) upon reexpression of wild-type Munc18-1–EmGFP. In contrast, the ability of K46E/E59K–EmGFP to rescue secretion was severely reduced, almost to the level of control EmGFP alone (Figure 7, A and B). Of interest, Munc18-1 K46E-EmGFP and E59K-EmGFP single mutants exhibited an intermediate level of secretion rescue that was significantly different from both wild-type Munc18-1–EmGFP and EmGFP alone (Figure 7, A and B). The single mutants failed to rescue secretion as prominently as that of wild-type Munc18-1–EmGFP but were capable of restoring the secretion defect significantly more than that of double mutants (Figure 7, A and B). The ability to restore secretion by these Munc18-1 mutants was in the order of WT > K46E ~ E59K >> K46E/E59K, which is again largely similar to the order of the abilities of these mutants to 1) bind syntaxin-1 and 2) restore its expression, suggesting a strong correlations among these variables. We illustrate more-detailed correlation analyses of these mutants together with other domain-1 cleft mutants (K63E, E66A, D34N, and D34N/M38V) in Figure 11 later in this paper.

K46E and E59K mutants display very similar phenotypes. Both of them partially lose their functions in syntaxin-1 binding, chaperoning, dense-core vesicle docking, and NA secretion. These results strongly imply that the priming function previously assigned to the E59K mutant is unlikely to completely explain the reduced secretion phenotypes of E59K. Our data point to a partial effect of the E59K mutation in syntaxin-1–chaperoning activity, similar to that seen with K46E. However, it was recently suggested that Vps33, a yeast SM protein, promotes fusion pore opening and that a homologous mutation in Vps33 to the E59K mutation in Munc18-1 abolishes this fusion pore opening function (Pieren *et al.*, 2010). We therefore examined whether there was a difference between K46E and E59K in their ability to rescue peptidergic secretion, as peptide secretion is suggested to require a more complete opening of the fusion pore (Barg *et al.*, 2002). We transfected the double-knockdown clones (D7 and D16) engineered to stably express Munc18-1 mutants (WT, K46E, E59K, or K46E/E59K) with a plasmid that allows the expression of neuropeptide Y(NPY) fused with a soluble domain (residues 18–506) of human placental alkaline phosphatase (NPY-hPLAP) and measured the stimulated secretion of this transfected peptide (Figure 7, C and D). NPY-PLAP is secreted in a Ca^{2+}-dependent manner (Fujita *et al.*, 2007; Han *et al.*, 2009), and both the levels of

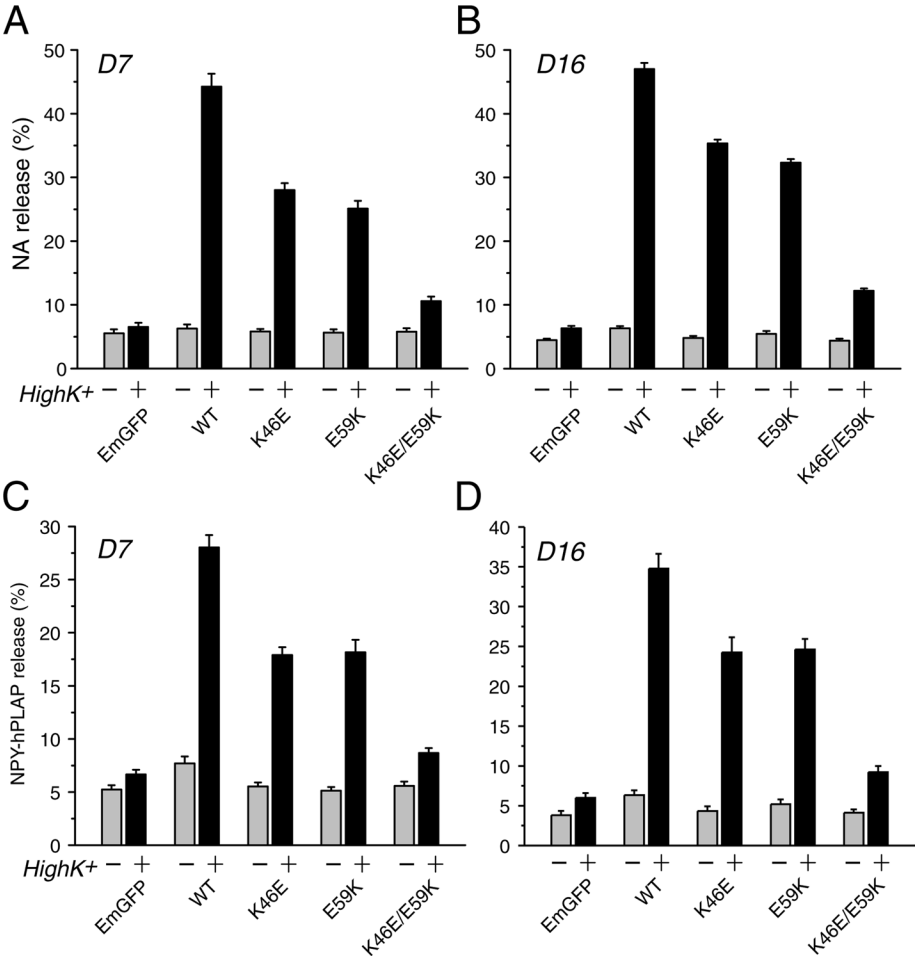

FIGURE 7: Secretion defects are rescued to different degrees upon reintroduction of Munc18-1 variants (K46E, E59K, and K46E/E59K) in Munc18-1/-2 double-knockdown cells. (A, B) NA release was stimulated by 70 mM KCl for 15 min in the rescued cells (A for D7 clones; B for D16 clones). Error bars indicate SEM (n = 12 for both D7 and D16). (C, D) Defects in peptide secretion in Munc18-1/-2 double-knockdown clones (D7 in C; D16 in D) were rescued to different extent upon reintroduction of Munc18-1 variants (K46E, E59K, and K46E/E59K). Secretion of transfected NPY-hPLAP from the double-knockdown clones expressing Munc18-1 variants was stimulated by 70 mM KCl for 25 min. Error bar, SEM (n = 11 for D7; n = 12 for D16).

NPY-hPLAP secreted from the cells and those retained in the cells are easily quantified by the heat-stable (65°C) alkaline phosphatase activity of hPLAP using a quantitative secretory alkaline phosphatase kit (*Materials and Methods*). We found that the secretory phenotypes of the peptide in these mutants are remarkably similar to that observed with NA release. Both E59K and K46E mutants showed reduced ability to secrete the transfected peptide when compared with the wild-type, whereas expression of the K46E/E59K mutant showed an abolished ability to rescue peptide secretion (Figure 7, C and D). The finding that the E59K does not exhibit a different phenotype from K46E in rescuing peptide secretion suggests that the E59K mutant does not specifically show selective defects in secretion that require a more complete opening of the fusion pore.

E66A and K63E mutants restore syntaxin-1 expression level, localization, and dense-core vesicle secretion as efficiently as the wild type in Munc18-1/-2 double-knockdown cells

Munc18-1 K63E and E66A single mutants were previously shown to retain strong binding to syntaxin-1, whereas E59K mutant showed a limited reduction in its binding to syntaxin-1 (Deák *et al*., 2009). In agreement with such results, our yeast two-hybrid result suggests that K63E and E66A mutants strongly retain the ability to bind to syntaxin-1 (Figure 1C). However, the chaperoning ability of these mutants was not addressed previously, and thus we further examined the ability of the K63E and E66A mutants to restore syntaxin-1 expression level and localization (Figure 8, A and C–E). Both of these domain-1 cleft mutants were capable of restoring syntaxin-1 expression and localization as efficiently as that of wild-type Munc18-1 (Figure 8, A and C–E). This strong rescuing activity of these mutants further supports our hypothesis that the binary interaction between Munc18-1 and syntaxin-1 is critical for the chaperoning activity of Munc18-1. After confirming intact chaperoning function of these domain-1 cleft mutants, we examined the ability of these mutants to restore the secretion defect in Munc18-1/-2 double–knockdown cells (Figure 8B). We found that both K63E and E66A mutants of Munc18-1 were capable of restoring the secretion defect in Munc18-1/-2 double–knockdown cells as efficiently as that of wild-type Munc18-1 (Figure 8B). Taken together, our results indicate that the degree of binary interaction with syntaxin-1 controls Munc18-1–chaperoning activity and, consequently, dense-core vesicle secretion.

Effect of Munc18-1 D34N and D34N/M38V on syntaxin-1 expression level and localization

In our yeast two-hybrid assays, the D34N single mutant modestly affects the binding to both syntaxin-1 and mint-1. The D34N/M38V mutant lost the ability to bind not only syntaxin-1, but also mint-1 (Figure 1, B and D). We therefore hypothesized that a misfolding of the D34N/M38V mutant (and potentially a less severe folding defect for the D34N single mutant) may have led to an inefficient expression of D34N/M38V protein. We examined the abilities of D34N and D34N/M38V mutants to rescue syntaxin-1 expression level and the localization to the plasma membrane in Munc18-1/-2 double-knockdown PC12 cells (Figures 9 and 10). In both D7 and D16 cells, Munc18-1 D34N mutant fused with EmGFP expressed at a comparable level to the endogenous Munc18-1, although slightly reduced compared with the expression level of WT Munc18-1–EmGFP (Figure 9, A and B). Moreover, this mutant was able to rescue syntaxin-1 expression, although not as efficiently as that of wild-type Munc18-1–EmGFP. Of interest, as we hypothesized, the D34N/M38V–EmGFP double mutant was unable to express well and, consequently, was incapable of restoring the syntaxin-1 expression level, which was similar to that of the Munc18-1/-2 double-knockdown cells alone or control cells expressing EmGFP alone (Figure 9, A and B). Similar to K46E and E59K, the ability of the D34N single mutant to restore the syntaxin-1 expression level can largely be explained by reduced binding to syntaxin-1 (Figure 1B) or reduced expression (Figure 9,

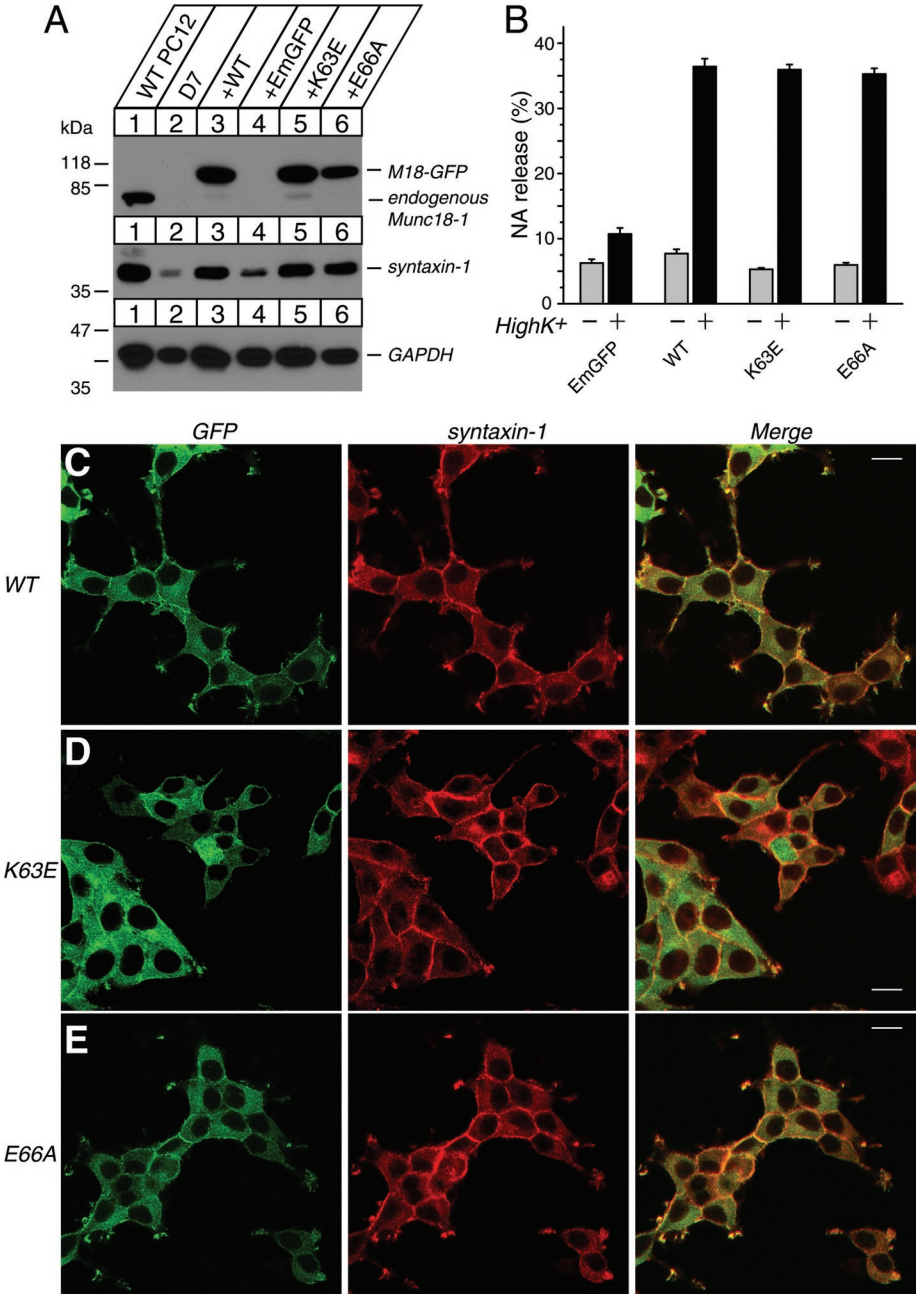

FIGURE 8: Syntaxin-1 expression level, syntaxin-1 localization, and secretion defect are restored upon stable reexpression of Munc18-1 K63E or E66A mutants in Munc18-1/-2 double-knockdown cells (D7). (A) Munc18-1/-2 double-knockdown clones (D7) were infected with lentiviruses that express EmGFP, wild-type Munc18-1–EmGFP, or Munc18-1 mutants (K63E, E66A), and the infected cells were selected with blasticidin. A number on the left indicates the position of a molecular weight marker. (B) NA release was stimulated by 70 mM KCl for 15 min in the rescued cells (D7 clones). Error bars indicate SEM (n = 9). (C–E) Confocal images of D7 cells infected with lentiviruses that express WT Munc18-1–EmGFP (C), K63E-EmGFP, (D) and E66A-EmGFP (E) (left). These cells were stained with anti–syntaxin-1 antibodies, followed by Red-X–conjugated anti-mouse antibodies (middle). Right, merged pictures. Bar, 10 μm.

A and B), which results in a defect in stabilizing the expression and localization of syntaxin-1. The inability of the D34N/M38V double mutant to restore the syntaxin-1 level is therefore likely to stem from its lack of expression.

We further confirmed the phenotype of these two mutants by examining their effects on syntaxin-1 localization, using confocal immunofluorescence microscopy (Figure 10). Expression of the D34N-EmGFP mutant in D16 cells rescued syntaxin-1 localization significantly (Figure 10B) but not as efficiently as that of the WT Munc18-1–EmGFP (Figure 10A). Although the plasma membrane localization of syntaxin-1 was prominent, intracellular accumulation of syntaxin-1 was also evident (Figure 10B). In the case of D34N/M38V-EmGFP–expressing cells, the EmGFP fluorescent signal for this mutant of Munc18-1 was barely detectable, indicating that the fusion protein was not adequately expressed (Figure 10C). Consequently, perinuclear accumulation of syntaxin-1 was observed in this double mutant (Figure 10C). Similar results were obtained for D7 cells (Supplemental Figure S2). These results are consistent with the immunoblot analysis (Figure 9, A and B), which revealed strikingly inefficient expression of D34N/M38V–EmGFP in double-knockdown cells.

Ability of D34N and D34N/M38V mutants to restore dense-core vesicle secretion in Munc18-1/-2 double-knockdown cells is also positively correlated with their syntaxin-1–chaperoning function

To further characterize the functional significance of D34N and D34N/M38V mutants, we performed [^{3}H]NA-release assay to study the effect of these mutants on secretion (Figure 9, C and D). The ability of the D34N-EmGFP mutant to rescue the secretion defect of Munc18-1/-2 double-knockdown cells was prominent compared with EmGFP control alone but was not as efficient as that of wild-type Munc18-1–EmGFP (Figure 9, C and D). This relatively strong rescuing ability of the D34N mutant is consistent with its relatively normal ability to bind syntaxin-1 and chaperoning activity (Figures 1, 9, and 10). This once again stresses the importance of the binary interaction between Munc18-1 and the closed conformation of syntaxin-1 on syntaxin-1 trafficking, which is crucial for neurosecretion. Furthermore, as expected, the D34N/M38V–EmGFP mutant exhibited limited ability to restore the secretion defect in double-knockdown cells, which is most likely because of its impaired expression (Figure 9, A and B). However, we also noted that the D34N/M38V mutant shows a more significant recovery of secretion in D16 cells compared with that in D7 cells (Figure 9, C and D). Of interest, the expression of D34N/M38V, as well as the recovery of syntaxin-1 level, indeed appeared to be higher in D16 cells than in D7 cells (Figures 9–11). The significant recovery of secretion by a small expression of D34N/M38V mutant in D16 cells also suggests that this mutant is unlikely to be a priming mutant.

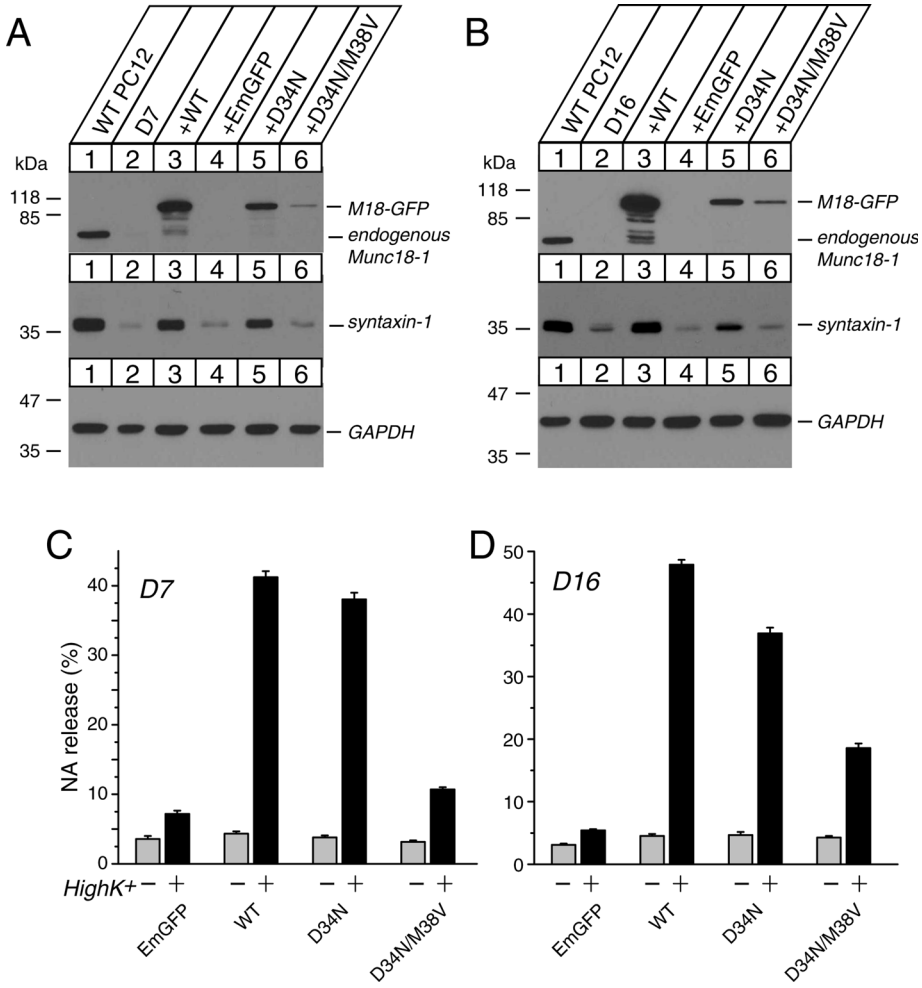

FIGURE 9: Stable reexpression of other domain-1 cleft (D34N, D34N/M38V) in Munc18-1/-2 double-knockdown PC12 cells (D7 and D16) and their effects on restoring noradrenaline secretion. (A, B) Munc18-1/-2 double-knockdown clones (D7 and D16) were infected with lentiviruses that express EmGFP, wild-type Munc18-1–EmGFP, or Munc18-1 mutants (D34N, D34N/M38V), and the infected cells were selected with blasticidin. A number on the left indicates the position of a molecular weight marker. (C, D) NA release was stimulated by 70 mM KCl for 15 min in the rescued cells (C for D7 clones; D for D16 clones). Error bars, SEM (n = 9 for both D7 and D16).

We finally examined the correlation between the ability of all of the domain-1 cleft mutants to restore syntaxin-1 expression and their ability to restore regulated secretion. Regulated secretion was calculated by subtracting NA release in PSS from high K^+–induced NA release and normalizing these values by those of the wild type, using the data shown in Figures 7–9. The regulated secretion observed in EmGFP-expressing D7 or D16 cells was subtracted from the regulated secretion of each mutant to more accurately estimate the restored regulated secretion (*y*-axis in Figure 11). In both D7 and D16 cells, there was a strong positive correlation between the restored syntaxin-1 expression and the restored regulated secretion, and these correlations were highly significant (D7: $r^2 = 0.93$, $p < 0.001$; D16: $r^2 = 0.73$, $p < 0.05$). Our results strongly indicate that the secretion defects exhibited by these mutants can largely be explained by their reduced ability to chaperone syntaxin-1.

DISCUSSION

In this study, we examined the role of Munc18-1's domain-1 cleft interaction with syntaxin-1 in neurosecretion by systematically investigating the contribution of this domain in the process of regulated exocytosis. We also reevaluated three mutants (E59K, E66A, and D34N/M38V) belonging to the domain-1 cleft, which were previously considered to affect Munc18-1 function during vesicle "priming." We generated and analyzed the phenotypes of an array of Munc18-1 domain-1 cleft mutants (K46E, E59K, K46E/E59K, K63E, E66A, D34N, and D34N/M38V) in rescuing syntaxin-1 expression (Figures 3, 8, and 9) and trafficking to the plasma membrane (Figures 4, 8, and 10). Moreover, we investigated the docking (Figures 5 and 6) and secretion phenotypes (Figures 7–9) of Munc18-1/-2 double-knockdown cells upon reexpression of these mutants. We discovered striking correlations between the abilities of these domain-1 cleft mutants to bind and chaperone syntaxin-1 and to restore the docking and secretion of dense-core vesicles (Figures 3C, 6D, and 11). Our results strongly suggest that domain-1 cleft of Munc18-1 contributes to exocytosis solely through its syntaxin-1–chaperoning function.

A previous study reported that the E59K and E66A single mutants exhibited significantly reduced ability to rescue the exocytosis defect in Munc18-1–deficient neurons compared with the wild-type and that the ability of these mutants to rescue exocytosis is correlated with their ability to bind the SNARE complex (Deák *et al.*, 2009). We found that the E59K mutant indeed reduces its ability to rescue secretion (Figures 7 and 11), whereas the E66A mutant can rescue secretion as effectively as the wild type (Figures 8 and 11). Our results also suggest that the secretory phenotype of the E59K mutant is better explained by its reduced chaperoning function of syntaxin-1. First, the combined results from both our yeast two-hybrid assays and ITC demonstrate a significant reduction in the binary interaction between the Munc18-1 E59K mutant and syntaxin-1 (Figures 1 and 2), which is consistent with another previous mutagenesis study that showed impaired binding between the E59K mutation in Munc18-2 and syntaxin-1–4 isoforms (Kauppi *et al.*, 2002). Deák *et al.* (2009) also found a significantly altered binding thermodynamics, with a greatly reduced enthalpic contribution to the association. Second, similar to K46E, E59K significantly loses the ability to restore syntaxin-1 expression (Figure 3) and localization (Figure 4). Third, K46E and E59K also exhibited similar levels of reductions in their ability to restore noradrenaline and peptide secretion (Figure 7). Our results strongly indicate that E59K is unlikely to have a specific deficit other than that in syntaxin-1 chaperoning.

The D34N/M38V double mutant has been considered to be another priming mutant (Gulyás-Kovács *et al.*, 2007). Despite significantly reduced binding to the closed conformation of syntaxin-1 and limited rescue of both impaired secretion and docking phenotypes in Munc18-1–null cells, this double mutant was shown to be able to significantly restore the syntaxin-1 pool. Our analysis of

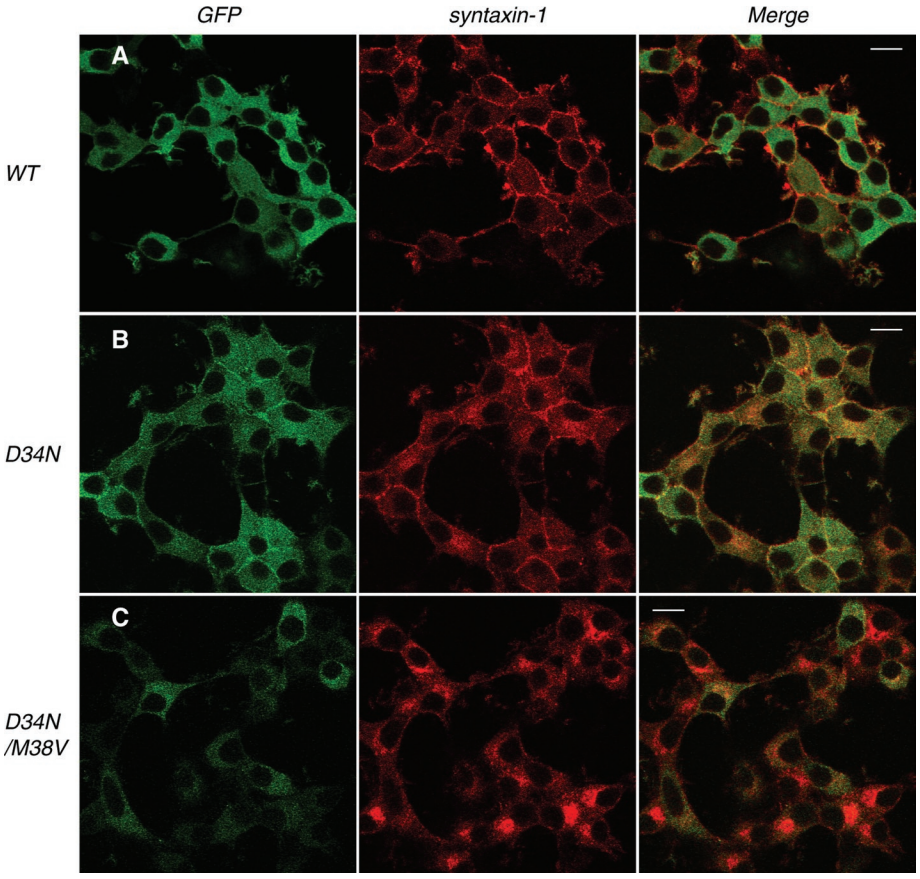

FIGURE 10: Syntaxin-1 localization in Munc18-1/-2 double-knockdown clone (D16) upon reintroduction of D34N and D34N/M38V Munc18-1 mutants. Confocal images of D16 cells infected with lentiviruses that express (A) wild-type Munc18-1–EmGFP, (B) D34N-EmGFP, and (C) D34N/M38V-EmGFP (left). These cells were stained with anti–syntaxin-1 antibodies, followed by Red-X–conjugated anti-mouse antibodies (middle). Right, merged pictures. Bar, 10 µm.

D34N/M38V, however, suggests that the inability of this mutant to rescue secretion of Munc18-1/-2–knockdown cells (Figure 9, C and D) is mainly due to its reduced binding to syntaxin-1 (Figure 1) caused by its inadequate expression (Figure 9, A and B), which results in an impaired syntaxin-1–chaperoning function (Figures 9 and 10). Our data are more consistent with previous work on Munc18-2 (Riento *et al.*, 2000), in which the same mutation in Munc18-2 strongly destabilized the expression of Munc18-2, resulting in the expression of ~20– 25% of WT. Moreover, the fact that a low expression of D34N/M38V mutant in D16 cells can still rescue NA secretion to certain degree (Figure 9D) excludes this double mutant from being a true priming mutant. Taken together, our results reveal that the reduced-secretion phenotypes observed in E59K and D34N/M38V mutants are more appropriately explained by their reduced syntaxin-1–chaperoning functions. Nevertheless, our findings still do not completely rule out a possible role of these Munc18-1 domain-1 cleft mutants in the priming stage of exocytosis in addition to the chaperoning function.

Another important function suggested for Munc18-1 is promoting vesicle docking. Severely impaired docking of the secretory granules was observed in Munc18-1–null chromaffin cells (Voets *et al.*, 2001). However, it has been controversial whether the defective vesicle docking in Munc18-1–null mutants is due to the direct contribution of Munc18-1 or is caused by an indirect effect of Munc18-1 through the regulation of the SNARE proteins, including syntaxin-1. The importance of syntaxin-1 in vesicle docking was demonstrated through the proteolytic cleavage of functional syntaxin by botulinum neurotoxin serotype C light chain, which led to an impaired-vesicle-docking phenotype (de Wit *et al.*, 2006). However, the contribution of Munc18-1 in this process remained elusive. In an attempt to fill this knowledge gap, we examined the ability of Munc18-1 K46E, E59K, and K46E/E59K mutants to rescue vesicle docking, through electron microscopic analysis (Figures 5 and 6). Our results revealed the same trend in rescuing ability of the mutants as for syntaxin-1 expression and localization. The trend of these results highlights a strong correlation between the ability of the mutants to rescue syntaxin-1 expression and trafficking and to restore vesicle docking (Figure 6D). This suggests that these two components of the exocytotic process are closely related. This strongly supports the idea that Munc18-1 contributes to vesicle docking through its regulation of syntaxin-1 by protecting and guiding syntaxin-1 so that syntaxin-1 can perform its function at the plasma membrane.

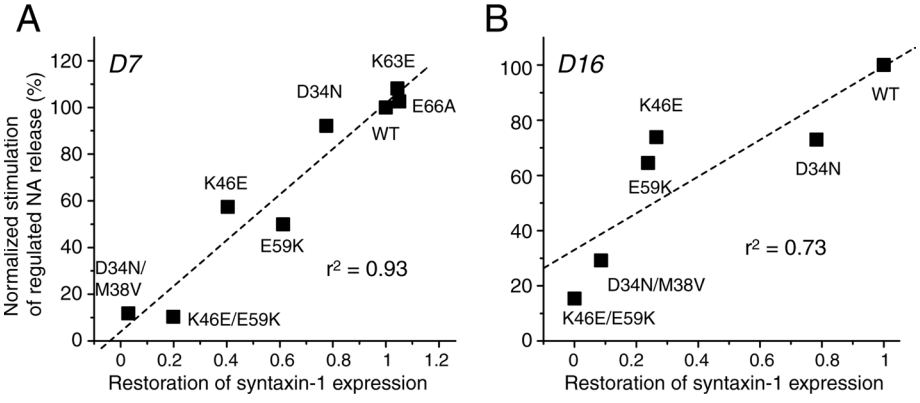

FIGURE 11: The ability of Munc18-1 mutants to restore syntaxin-1 and the ability to restore regulated secretion are positively correlated. The correlation graph demonstrates the positive correlation between the ability of the domain-1 cleft mutants to restore syntaxin-1 expression level and the ability to rescue regulated NA secretion defect.

In addition to E59K, E66A, and D34N/M38V, two other mutants (F115R, Y337L) have been suggested to specifically affect synaptic vesicles priming in exocytosis (Boyd *et al.*, 2008; Johnson *et al.*, 2009). Phe115 belongs to the hydrophobic domain of Munc18-1 and interacts with the N-terminal peptide of syntaxin-1 (Hu *et al.*, 2007; Burkhardt *et al.*, 2008). The function of the N-terminal binding mode in

membrane fusion/exocytosis is conflicting. In *C. elegans*, the F113R mutant in UNC-18 (corresponds to the F115R mutation in Munc18-1) could not rescue the locomotion defects seen in the UNC-18–null phenotype, whereas two recent reports revealed that inhibiting the N-terminal binding between Munc18-1 and syntaxin-1 in PC12 cells only has a limited impact on dense-core vesicle exocytosis (Han *et al.*, 2009; Malintan *et al.*, 2009). Besides domain-1, domain-3a of Munc18-1 is also believed to be important for syntaxin-1 interaction. Recently, it was suggested that Munc18-1 domain-3a undergoes a conformational change that might allow coiled-coil interactions with SNARE complexes (Hu *et al.*, 2011). Another study reported the functional importance of domain-3a in the membrane fusion process by characterizing the Munc18-1 Y337L mutation. On overexpression, Y337L acts as a dominant-negative mutant, which results in slowed and prolonged release of catecholamine from individual vesicles (Boyd *et al.*, 2008). However, our recent results suggest that the Munc18-1 Y337L mutant retains completely intact binding to the closed conformation of syntaxin-1 and that this mutant is actually capable of restoring both syntaxin-1 expression level and the dense-core vesicle secretion defect in Munc18-1/-2 double-knockdown cells as efficiently as that of wild type (unpublished data). Therefore further studies are required to investigate the functional significance of different domains of Munc18-1 in neurosecretion. It is surprising that no true priming mutant that selectively impairs the priming stage of exocytosis without affecting its syntaxin-1 chaperoning function has yet been discovered. The discovery of such a mutant(s) will certainly advance our understanding of Munc18-1–dependent stimulation/priming of membrane fusion at the molecular level.

MATERIALS AND METHODS

General materials

Parental pLVX-IRES-puro plasmid for *Lentivirus*-mediated Munc18-1 expression was purchased from Clontech Laboratories (Mountain View, CA). psPAX2 was purchased from Addgene (Cambridge, MA), and pMD2G was a kind gift from Tomoyuki Mashimo (University of Texas Southwestern Medical Center at Dallas, Dallas, TX). We obtained monoclonal antibodies against syntaxin-1 (clone HPC-1) (Barnstable *et al.*, 1985) from Sigma-Aldrich Canada (Oakville, Canada); Munc18-1 was from BD Biosciences (Mississauga, Canada), and glyceraldehyde-3-phosphate dehydrogenase (clone 6C5) was from Millipore (Billerica, MA).

Lentivirus-mediated expression of Munc18-1 variants in Munc18-1/-2 double-knockdown cells

Two clonal lines of Munc18-1/2 double-knockdown cells (D7, D16) were maintained in DMEM (Invitrogen, Carlsbad, CA) containing 5% calf serum, 5% horse serum (both from HyClone Laboratories, Logan, UT), penicillin (100 U/ml)/streptomycin (0.1 mg/ml) (Sigma-Aldrich Canada), 250 ng/ml amphotericin B (Sigma-Aldrich Canada), puromycin (2.5 μg/ml), and G418 (700 μg/ml). We generated the *Lentivirus*-mediated expression constructs of various Munc18-1 mutants so that these proteins stably express in the Munc18-1/-2 double-knockdown cells. The parental expression plasmid was developed by modifying pLVX-IRES-puro. First, the puromycin-resistance gene was replaced by a blasticidin-resistance gene so that the infected cells could be selected with blasticidin. Second, cDNA sequence for EmGFP was subcloned into the *Bam*HI site, generating pLVX-EmGFP-IRES-blast. In our previous articles (Arunachalam *et al.*, 2008; Han *et al.*, 2009), we introduced six silent nucleotide mutations (SNMs) (GTCCGTGCACAGCCTGATC; underlines indicate SNM) within the target sequence in the Munc18-1 gene to protect the mRNA transcripts transcribed from the Munc18-1 expression plasmid from being degraded by the anti–Munc18-1 RNA interference machineries already introduced within the Munc18-1/-2 double-knockdown cells. The Munc18-1 (SNM) gene (WT or its indicated mutant) digested from pLCMV-Munc18-1 (SNM)-EmGFP-blast (Han *et al.*, 2009) with *Eco*RI/*Xba*I was subcloned into the same site of the pLVX-EmGFP-IRES-blast plasmid. This Munc18-1 expression plasmid was cotransfected with psPAX2 and pMD2G into HEK-293FT cells to generate recombinant lentiviruses that express Munc18-1 WT or its variant fused with EmGFP. The Munc18-1/-2 double-knockdown cells that were infected with lentiviruses expressing rescue proteins were selected with blasticidin (5 μg/ml).

Yeast two-hybrid assays

Full-length WT Munc18-1 with SNM (see preceding section) or indicated mutant Munc18-1 (SNM) was subcloned into the *Sma*I-*Pst*I site of a bait vector, pLexN. A cytoplasmic domain (residues 1–264) of rat syntaxin-1A and residues 129–451 of rat mint-1, which contains a Munc18-1–interacting domain (residues 226–314; Okamoto and Südhof, 1997), were subcloned into the *Eco*RI–*Bgl*II site of a prey vector, pVP16-3 (Okamoto and Südhof, 1997). Yeast strain L40 (Vojtek *et al.*, 1993) was transfected with bait and prey vectors by using the lithium acetate method (Schiestl and Gietz, 1989). Transformants were plated on selection plates lacking uracil, tryptophan, and leucine. After 2 d of incubation at 30°C, colonies were inoculated into supplemented minimal medium lacking uracil, tryptophan, and leucine and placed in a shaking incubator at 30°C for 2 d.

β-Galactosidase assays were performed as follows. Yeast cells were chilled on ice and harvested by centrifugation (2000 rpm for 5 min). The collected yeast cells were resuspended in 250 μl of breaking buffer (100 mM Tris-Cl, pH 8.0, 1 mM dithiothreitol [DTT], and 20% glycerol). Then, glass beads (0.45–0.5 mm; Sigma Chemical) were added to the yeast suspension to a level just below the meniscus of the liquid, followed by 12.5 μl of phenylmethylsulfonyl fluoride stock solution (40 mM in 100% isopropanol stored at −20°C). The mixture was then vortexed six times at top speed in15-s bursts. After that, another 250 μl of breaking buffer was added, mixed well, and centrifuged for 1 min. The liquid extract was withdrawn and transferred to new tubes. The extracted liquid was further clarified by centrifuging for 15 min in a microcentrifuge. To perform the assay, 80 μl of the extract was added to 720 μl of Z buffer (60 mM Na_2HPO_4, 40 mM NaH_2PO_4, 10 mM KCl, 1 mM $MgSO_4$, and 2.7 ml/l β-mercaptoethanol, pH 7.0). The mixture was then incubated in a water bath at room temperature for 5 min. The reaction was initiated by adding 0.16 ml of stock solution (4 mg/ml *o*-nitrophenyl-β-D-galactoside in Z buffer; −20°C), and the reaction mixture was incubated at room temperature. The reaction was precisely terminated at the end of 7-min incubation by addition of 0.4 ml of 1 M Na_2CO_3 stock solution in distilled water, and the optical density of the reaction mixture was measured at 420 nm by using a spectrophotometer. At the same time, the protein concentration in the extract was measured using Bradford dye-binding assay. A standard curve was prepared using serial dilutions of bovine serum albumin dissolved in breaking buffer. Ten milliliters of the extract were added to 1 ml of the Bradford reagent (Bio-Rad Laboratories, Hercules, CA), and the change in color was measured at 595 nm by using a spectrophotometer. The specific activity of β-galactosidase in the extract was calculated according to the following formula: (OD_{420} × 1.36)/(0.0045 × protein concentration [mg/ml] × extract volume [0.08 ml] × 7 min), where OD_{420} is the

optical density of the product *o*-nitrophenol at 420 nm. The factor 1.36 corrects for the reaction volume, and the factor 0.0045 is the optical density of 1 nmol/ml solution of *o*-nitrophenol. The unit of β-galactosidase–specific activity is therefore expressed as nanomoles per minute per milligram of protein.

Isothermal titration calorimetry

Recombinant proteins Syntaxin1a$_{2\text{-}243}$ and Munc18-1-WT or mutants used for the ITC experiments were prepared as previously described (Malintan *et al*. 2009). All proteins were further purified by gel filtration chromatography using 20 mM sodium phosphate buffer (pH 7.5), 150 mM NaCl, and 1 mM DTT (ITC buffer). Isothermal titration calorimetry was carried out at 298 K using a MicroCal iTC200 (GE Healthcare, Chalfont St Giles, United Kingdom), with 16× 2.4-µl injections of 70 µM Syntaxin1a$_{2\text{-}243}$ into 7 µM Munc18-1-WT or mutants. Integration of the titration curves was performed using the ORIGIN software (OriginLab, Northampton, United Kingdom) to extract thermodynamic parameters, stoichiometry N, equilibrium association constant K_a (= K_d^{-1}), and the binding enthalpy ΔH. The Gibbs free energy of binding ΔG was calculated from the relation $\Delta G = -RT \ln(K_a)$, and the binding entropy ΔS was deduced from the equation ($\Delta G = \Delta H - T\Delta S$). Experiments were performed with protein concentrations well within the recommended range for the c value (concentration of protein in cell/K_d ~ 200). Binding parameters were calculated as the average of at least three independent experiments ± SD.

Cell preparation for confocal immunofluorescence microscopy

Sterilized circular glass coverslips (0.25 mm in width, 1.8 cm in diameter) were placed in 2.2-cm wells within 12-well cell culture plates. The coverslips were then coated for 1 h with poly-D-lysine (0.1 mg/ml) at room temperature. Cells were allowed to adhere to the coverslips overnight and then differentiated on the coverslips for 3–4 d in DMEM that contained 100 ng/ml nerve growth factor (Sigma-Aldrich), 1% horse serum, 1% calf serum, and penicillin/streptomycin. The cells were washed with phosphate-buffered saline (PBS) and fixed for 15 min with PBS containing 4% paraformaldehyde (PFA). PFA was then removed from each well, and cells were rinsed three times (10 min each time) with 1 ml of PBS per well. The fixed cells were then permeabilized with PBS containing 0.2% Triton X-100 and 0.3% bovine serum albumin (BSA) for 5 min, followed by three washes with PBS. Nonspecific sites were blocked for 1 h at room temperature in PBS containing 0.3% BSA. Primary antibodies against syntaxin-1 (HPC-1 diluted 1:1000) were applied to the cell for 1 h. After three washes in blocking buffer, Rhodamine Red-X–conjugated anti-mouse antibodies (diluted 1:1000; Jackson ImmunoResearch Laboratories, West Grove, PA) were applied for 1 h. Samples were washed again three times in blocking buffer and mounted in Fluoromount-G reagent (Southern Biotechnology, Birmingham, AL). Immunofluorescence staining was recorded with a laser confocal scanning microscope (LSM510; Carl Zeiss, Jena, Germany) with an oil immersion objective lens (63×).

Electron microscopy and analysis of docking of dense-core vesicles

The initial fixation was performed within the 10-cm dishes for 1 h using a 3.2% glutaraldehyde and 2.5% paraformaldehyde fixative mixture (Karnovsky's fixative) in 0.1 M cacodylate buffer (pH adjusted to 7.6). Cells were then pelleted in microcentrifuge tubes and fixed overnight with new fixative. The following day, the pellets were fixed in 1 mg/ml (1%) osmium tetroxide for 1 h, and en bloc staining was then performed by incubating with 1% uranyl acetate for 1 h in dark conditions. Washed pellets were incubated successively in increasing concentrations of ethanol for dehydration and then infiltrated overnight with Spurr's resin (23.6 g of NSA, 16.4 g of ERL-4221, 5.72 g of DER-736, and 0.4 g of DMAE). After transferal of the cell pellets to Beem capsules, the capsules were incubated for 48 h at 65°C. The plasticized pellets were sliced to ultrathin 80-nm sections, which were then mounted on copper grids for subsequent staining and viewing.

Grids mounted with the ultrathin cell sections were first etched by exposing the grids to 3% uranyl acetate for 45 min at room temperature. Grids were then washed and stained with lead citrate for 20 min. Grids were washed and dried again before loading onto a Hitachi H7000 transmission electron microscope for viewing. Electron micrographs were taken of individual cells within each type of control or Munc18-1/-2 double-knockdown cells expressing K46E, E59K, or K46E/E59K mutant. These images were then used for analyzing the docking of dense-core vesicles in the control or the Munc18-1 variants expressing PC12 cells. Dense-core vesicles were identified within the single-cell electron micrographs as dark spots of radius between 60 and 120 nm. The distance of each vesicle from the plasma membrane was then calculated for each individual cell. The data from multiple single-cell images (n = 37–40) within each control or Munc18-1 variants were collated.

[^{3}H]Noradrenaline release assays from PC12 cells

PC12 cells were plated in 24-well plates; 3–4 d after plating, the cells were labeled with 0.5 µCi of [^{3}H]NA in the presence of 0.5 mM of ascorbic acid for 12–16 h. The labeled PC12 cells were incubated with the fresh complete DMEM for 1–5 h to remove unincorporated [^{3}H]NA. The cells were washed once with physiological saline solution (PSS) containing 145 mM NaCl, 5.6 mM KCl, 2.2 mM $CaCl_2$, 0.5 mM $MgCl_2$, 5.6 mM glucose, and 15 mM 4-(2-hydroxyethyl)-1-piperazineethanesulfonic acid, pH 7.4, and NA secretion was stimulated with 200 µl of PSS or high-K^+ PSS (containing 81 mM NaCl and 70 mM KCl). Secretion was terminated after a 15-min incubation at 37°C by chilling to 0°C, and samples were centrifuged at 4°C for 3 min. Supernatants were removed, and the pellets were solubilized in 0.1% Triton X-100 for liquid scintillation counting.

hPLAP secretion assay from PC12 cells

Munc18-1/-2 double-knockdown PC12 cells that stably express wild-type Munc18-1 or Munc18-1 variants were transfected with 3 µg of a reporter plasmid, pCMV-NPY-hPLAP, by using electroporation (Fujita *et al*., 2007; Li *et al*., 2007; Arunachalam *et al*., 2008) when the cells were at 70–80% confluency in 10-cm dishes. After 48 h, the cells were harvested and replated in 24-well plates. At 6 or 7 d after electroporation, the plated cells were washed once with PSS. Then NPY-hPLAP secretion was stimulated with 200 µl of PSS or high-K^+ PSS. Secretion was terminated after a 25-min incubation at 37°C by chilling to 0°C, and samples were centrifuged at 4°C for 3 min. Supernatants were removed, and the pellets were solubilized in 200 µl of PSS containing 0.1% Triton X-100. The amounts of NPY-hPLAP secreted into the medium and retained in the cell were measured by the Phospha-Light Reporter Gene Assay System (Applied Biosystems, Foster City, CA). We treated the samples at 65°C for 30 min to inactivate nonplacental alkaline phosphatases and assayed an aliquot (10 µl) for placental alkaline phosphatase activity with the kit. The total volume of the assay was 120 µl. After 5–10 min, chemiluminescence was quantified by an FB12 luminometer (Berthold Detection Systems, Zylux, Oak Ridge, TN).

ACKNOWLEDGMENTS

This research was supported by the Canada Research Chair Program, the Heart and Stroke Foundation (Grants NA6217 and T6700), the Natural Sciences and Engineering Research Council of Canada (Grant 456042), the Canadian Institute of Health Research (MOP-93665), a grant from the National Health and Medical Research Council of Australia (to B.M.C. and F.A.M.), and a fellowship to F.A.M. from the National Health and Medical Research Council of Australia. B.M.C. is supported by an Australian Research Council Future Fellowship (FT100100027). We thank Jasmine Davis for assistance with expression and purification of recombinant proteins.

REFERENCES

Arunachalam L *et al.* (2008). Munc18-1 is critical for plasma membrane localization of syntaxin1 but not of SNAP-25 in PC12 cells. Mol Biol Cell 19, 722–734.

Barg S, Olofsson CS, Schriever-Abeln J, Wendt A, Gebre-Medhin S, Renström E, Rorsman P (2002). Delay between fusion pore opening and peptide release from large dense-core vesicles in neuroendocrine cells. Neuron 33, 287–299.

Barnstable CJ, Hofstein R, Akagawa K (1985). A marker of early amacrine cell development in rat retina. Brain Res 352, 286–290.

Boyd A, Ciufo LF, Barclay JW, Graham ME, Haynes LP, Doherty MK, Riesen M, Burgoyne RD, Morgan A (2008). A random mutagenesis approach to isolate dominant-negative yeast sec1 mutants reveals a functional role for domain 3a in yeast and mammalian Sec1/Munc18 proteins. Genetics 180, 165–178.

Bracher A, Perrakis A, Dresbach T, Betz H, Weissenhorn W (2000). The X-ray crystal structure of neuronal Sec1 from squid sheds new light on the role of this protein in exocytosis. Structure 8, 685–694.

Bracher A, Weissenhorn W (2001). Crystal structures of neuronal squid Sec1 implicate inter-domain hinge movement in the release of t-SNAREs. J Mol Biol 306, 7–13.

Burkhardt P, Hattendorf DA, Weis WI, Fasshauer D (2008). Munc18a controls SNARE assembly through its interaction with the syntaxin N-peptide. EMBO J 27, 923–933.

de Wit H, Cornelisse LN, Toonen RF, Verhage M (2006). Docking of secretory vesicles is syntaxin dependent. PLoS One 1, e126.

Deák F, Xu Y, Chang WP, Dulubova I, Khvotchev M, Liu X, Südhof TC, Rizo J (2009). Munc18-1 binding to the neuronal SNARE complex controls synaptic vesicle priming. J Cell Biol 184, 751–764.

Dulubova I, Khvotchev M, Liu S, Huryeva I, Südhof TC, Rizo J (2007). Munc18-1 binds directly to the neuronal SNARE complex. Proc Natl Acad Sci USA 104, 2697–2702.

Fujita Y *et al.* (2007). Ca2+-dependent activator protein for secretion 1 is critical for constitutive and regulated exocytosis but not for loading of transmitters into dense core vesicles. J Biol Chem 282, 21392–21403.

Garcia EP, Gatti E, Butler M, Burton J, De Camilli P (1994). A rat brain Sec1 homologue related to Rop and UNC18 interacts with syntaxin. Proc Natl Acad Sci USA 91, 2003–2007.

Gulyás-Kovács A, de Wit H, Milosevic I, Kochubey O, Toonen R, Klingauf J, Verhage M, Sørensen JB (2007). Munc18-1: sequential interactions with the fusion machinery stimulate vesicle docking and priming. J Neurosci 27, 8676–8686.

Halachmi N, Lev Z (1996). The Sec1 family: a novel family of proteins involved in synaptic transmission and general secretion. J Neurochem 66, 889–897.

Han G, Malintan N, Collins B, Meunier F, Sugita S (2010). Munc18-1 as a key regulator of neurosecretion. J Neurochem.

Han L *et al.* (2009). Rescue of Munc18-1 and -2 double knockdown reveals the essential functions of interaction between Munc18 and closed syntaxin in PC12 cells. Mol Biol Cell 20, 4962–4975.

Hata Y, Slaughter CA, Südhof TC (1993). Synaptic vesicle fusion complex contains unc-18 homologue bound to syntaxin. Nature 366, 347–351.

Hata Y, Südhof T (1995). A novel ubiquitous form of Munc-18 interacts with multiple syntaxins. Use of the yeast two-hybrid system to study interactions between proteins involved in membrane traffic. J Biol Chem 270, 13022–13028.

Hosono R, Hekimi S, Kamiya Y, Sassa T, Murakami S, Nishiwaki K, Miwa J, Taketo A, Kodaira KI (1992). The unc-18 gene encodes a novel protein affecting the kinetics of acetylcholine metabolism in the nematode *Caenorhabditis elegans*. J Neurochem 58, 1517–1525.

Hu SH, Christie MP, Saez NJ, Latham CF, Jarrott R, Lua LH, Collins BM, Martin JL (2011). Possible roles for Munc18-1 domain 3a and Syntaxin1 N-peptide and C-terminal anchor in SNARE complex formation. Proc Natl Acad Sci USA 108, 1040–1045.

Hu SH, Latham CF, Gee CL, James DE, Martin JL (2007). Structure of the Munc18c/Syntaxin4 N-peptide complex defines universal features of the N-peptide binding mode of Sec1/Munc18 proteins. Proc Natl Acad Sci USA 104, 8773–8778.

Johnson JR, Ferdek P, Lian LY, Barclay JW, Burgoyne RD, Morgan A (2009). Binding of UNC-18 to the N-terminus of syntaxin is essential for neurotransmission in *Caenorhabditis elegans*. Biochem J 418, 73–80.

Katagiri H, Terasaki J, Murata T, Ishihara H, Ogihara T, Inukai K, Fukushima Y, Anai M, Kikuchi M, Miyazaki J (1995). A novel isoform of syntaxin-binding protein homologous to yeast Sec1 expressed ubiquitously in mammalian cells. J Biol Chem 270, 4963–4966.

Kauppi M, Wohlfahrt G, Olkkonen VM (2002). Analysis of the Munc18b-syntaxin binding interface. Use of a mutant Munc18b to dissect the functions of syntaxins 2 and 3. J Biol Chem 277, 43973–43979.

Latham CF *et al.* (2006). Molecular dissection of the Munc18c/syntaxin4 interaction: implications for regulation of membrane trafficking. Traffic 7, 1408–1419.

Latham CF, Meunier FA (2007). Munc18a: Munc-y business in mediating exocytosis. Int J Biochem Cell Biol 39, 1576–1581.

Li G *et al.* (2007). RalA and RalB function as the critical GTP sensors for GTP-dependent exocytosis. J Neurosci 27, 190–202.

Malintan NT, Nguyen TH, Han L, Latham CF, Osborne SL, Wen PJ, Lim SJ, Sugita S, Collins BM, Meunier FA (2009). Abrogating Munc18-1-SNARE complex interaction has limited impact on exocytosis in PC12 cells. J Biol Chem 284, 21637–21646.

McEwen JM, Kaplan JM (2008). UNC-18 promotes both the anterograde trafficking and synaptic function of syntaxin. Mol Biol Cell 19, 3836–3846.

Medine CN, Rickman C, Chamberlain LH, Duncan RR (2007). Munc18-1 prevents the formation of ectopic SNARE complexes in living cells. J Cell Sci 120, 4407–4415.

Misura KM, Scheller RH, Weis WI (2000). Three-dimensional structure of the neuronal-Sec1-syntaxin 1a complex. Nature 404, 355–362.

Okamoto M, Südhof TC (1997). Mints, Munc18-interacting proteins in synaptic vesicle exocytosis. J Biol Chem 272, 31459–31464.

Pevsner J, Hsu SC, Scheller RH (1994). n-Sec1: a neural-specific syntaxin-binding protein. Proc Natl Acad Sci USA 91, 1445–1449.

Pieren M, Schmidt A, Mayer A (2010). The SM protein Vps33 and the t-SNARE H(abc) domain promote fusion pore opening. Nat Struct Mol Biol 17, 710–717.

Rathore SS, Bend EG, Yu H, Hammarlund M, Jorgensen EM, Shen J (2010). Syntaxin N-terminal peptide motif is an initiation factor for the assembly of the SNARE-Sec1/Munc18 membrane fusion complex. Proc Natl Acad Sci USA 107, 22399–22406.

Rickman C, Medine CN, Bergmann A, Duncan RR (2007). Functionally and spatially distinct modes of munc18-syntaxin 1 interaction. J Biol Chem 282, 12097–12103.

Riento K, Galli T, Jansson S, Ehnholm C, Lehtonen E, Olkkonen VM (1998). Interaction of Munc-18-2 with syntaxin 3 controls the association of apical SNAREs in epithelial cells. J Cell Sci 111 (Pt 17), 2681–2688.

Riento K, Jäntti J, Jansson S, Hielm S, Lehtonen E, Ehnholm C, Keränen S, Olkkonen VM (1996). A sec1-related vesicle-transport protein that is expressed predominantly in epithelial cells. Eur J Biochem 239, 638–646.

Riento K, Kauppi M, Keranen S, Olkkonen VM (2000). Munc18-2, a functional partner of syntaxin 3, controls apical membrane trafficking in epithelial cells. J Biol Chem 275, 13476–13483.

Rizo J, Südhof TC (2002). Snares and Munc18 in synaptic vesicle fusion. Nat Rev Neurosci 3, 641–653.

Rodkey TL, Liu S, Barry M, McNew JA (2008). Munc18a scaffolds SNARE assembly to promote membrane fusion. Mol Biol Cell 19, 5422–5434.

Rowe J, Calegari F, Taverna E, Longhi R, Rosa P (2001). Syntaxin 1A is delivered to the apical and basolateral domains of epithelial cells: the role of munc-18 proteins. J Cell Sci 114, 3323–3332.

Rowe J, Corradi N, Malosio ML, Taverna E, Halban P, Meldolesi J, Rosa P (1999). Blockade of membrane transport and disassembly of the Golgi complex by expression of syntaxin 1A in neurosecretion-incompetent cells: prevention by rbSEC1. J Cell Sci 112 (Pt 12), 1865–1877.

Schiestl RH, Gietz RD (1989). High efficiency transformation of intact yeast cells using single stranded nucleic acids as a carrier. Curr Genet 16, 339–346.

Schulze KL, Littleton JT, Salzberg A, Halachmi N, Stern M, Lev Z, Bellen HJ (1994). rop, a *Drosophila* homolog of yeast Sec1 and vertebrate n-Sec1/Munc-18 proteins, is a negative regulator of neurotransmitter release in vivo. Neuron 13, 1099–1108.

Shen J, Rathore S, Khandan L, Rothman J (2010). SNARE bundle and syntaxin N-peptide constitute a minimal complement for Munc18-1 activation of membrane fusion. J Cell Biol 190, 55–63.

Shen J, Tareste D, Paumet F, Rothman J, Melia T (2007a). Selective activation of cognate SNAREpins by Sec1/Munc18 proteins. Cell 128, 183–195.

Shen J, Tareste DC, Paumet F, Rothman JE, Melia TJ (2007b). Selective activation of cognate SNAREpins by Sec1/Munc18 proteins. Cell 128, 183–195.

Südhof TC, Rothman JE (2009). Membrane fusion: grappling with SNARE and SM proteins. Science 323, 474–477.

Tamori Y, Kawanishi M, Niki T, Shinoda H, Araki S, Okazawa H, Kasuga M (1998). Inhibition of insulin-induced GLUT4 translocation by Munc18c through interaction with syntaxin4 in 3T3-L1 adipocytes. J Biol Chem 273, 19740–19746.

Tareste D, Shen J, Melia T, Rothman J (2008). SNAREpin/Munc18 promotes adhesion and fusion of large vesicles to giant membranes. Proc Natl Acad Sci USA 105, 2380–2385.

Tellam JT, Macaulay SL, McIntosh S, Hewish DR, Ward CW, James DE (1997). Characterization of Munc-18c and syntaxin-4 in 3T3-L1 adipocytes. Putative role in insulin-dependent movement of GLUT-4. J Biol Chem 272, 6179–6186.

Tellam JT, McIntosh S, James DE (1995). Molecular identification of two novel Munc-18 isoforms expressed in non-neuronal tissues. J Biol Chem 270, 5857–5863.

Toonen RF, Kochubey O, de Wit H, Gulyas-Kovacs A, Konijnenburg B, Sørensen JB, Klingauf J, Verhage M (2006). Dissecting docking and tethering of secretory vesicles at the target membrane. EMBO J 25, 3725–3737.

Toonen RF, Verhage M (2007). Munc18-1 in secretion: lonely Munc joins SNARE team and takes control. Trends Neurosci 30, 564–572.

Verhage M *et al*. (2000). Synaptic assembly of the brain in the absence of neurotransmitter secretion. Science 287, 864–869.

Voets T, Toonen RF, Brian EC, de Wit H, Moser T, Rettig J, Südhof TC, Neher E, Verhage M (2001). Munc18-1 promotes large dense-core vesicle docking. Neuron 31, 581–591.

Vojtek A, Hollenberg S, Cooper J (1993). Mammalian Ras interacts directly with the serine/threonine kinase Raf. Cell 74, 205–214.

Weimer RM, Richmond JE, Davis WS, Hadwiger G, Nonet ML, Jorgensen EM (2003). Defects in synaptic vesicle docking in unc-18 mutants. Nat Neurosci 6, 1023–1030.

Xu Y, Su L, Rizo J (2010). Binding of Munc18-1 to synaptobrevin and to the SNARE four-helix bundle. Biochemistry 49, 1568–1576.